Short range force effects in semiclassical molecular line broadening calculations

D. Robert, J. Bonamy

Tome 40 N° 10 OCTOBRE 1979

LE JOURNAL DE PHYSIQUE

Classification
Physics Abstracts
33.20E — 33.20F — 33.70 — 34.20

Short range force effects in semiclassical molecular line broadening calculations

D. Robert and J. Bonamy

Laboratoire de Physique Moléculaire (*), Faculté des Sciences et des Techniques, 25030 Besançon Cedex, France

(*Reçu le 26 mars 1979, accepté le 12 juin 1979*)

Résumé. — Une théorie semi-classique de l'élargissement et du déplacement des raies infrarouge et Raman en phase gazeuse est développée dans le cadre de l'approximation d'impact. Un modèle de trajectoire parabolique, pilotée par la partie isotrope du potentiel intermoléculaire, permet un traitement satisfaisant des collisions à courte approche tout en conservant une formulation analytique de la section de collision élastique. Nous avons testé cette théorie en comparant nos résultats, pour le cas HCl-Ar, aux résultats d'autres auteurs qui utilisaient un traitement à l'ordre infini et des trajectoires classiques numériques. Les calculs ont ensuite été étendus au cas des collisions diatome-diatome, en exprimant le potentiel d'interaction anisotrope à l'aide d'un modèle *atome-atome*, lequel tient compte à la fois des contributions à longue et à courte distance. Des applications numériques ont été réalisées pour les raies Raman des gaz purs N_2, CO_2 et CO et pour les raies infrarouges de CO autoperturbé et perturbé par N_2 et CO_2. Dans tous les cas, nous avons obtenu un bon accord quantitatif avec l'expérience, et en particulier les variations de la largeur de raie avec le nombre quantique rotationnel ont été correctement reproduites, même à basse température, ce qui n'était pas le cas dans les travaux antérieurs.

Abstract. — A semiclassical theory of the width and shift of isolated infrared and Raman lines in the gas phase is developed within the impact approximation. A parabolic trajectory model determined by the isotropic part of the interaction potential allows a satisfactory treatment to be made of the close collisions leading to an analytical expression for the elastic collision cross section. A numerical test of this theory has been made for HCl-Ar by comparing the present results to those of previous infinite order treatments using numerical curved classical trajectories. Extension to the diatom-diatom collisions is then made by expressing the anisotropic potential using an atom-atom interaction model which takes both the long and short range contributions into account. Numerical applications have been performed for the Raman line widths of pure N_2, CO_2 and CO and for the infrared line widths of pure CO and of CO perturbed by N_2 and CO_2. A good quantitative agreement with experiments is obtained for all the considered cases and a correct variation of the broadening coefficient with the rotational quantum number is achieved in opposition to the previous results. A consistent variation of the line broadening with temperature is also obtained even for high rotational levels.

1. **Introduction.** — The most broadly applied theory of pressure broadening of isolated spectral lines is that developed by Anderson [1], which has been systematized by Tsao and Curnutte [2] and extended to the Raman lines by Fiutak and van Kranendonk [3]. In fact this perturbative treatment leads to reasonable agreement with experiments only if molecular gases for which a strong dipolar interaction exists [4-6] are considered. Indeed, in this case, the optical collision diameter is always higher than the kinetic collision diameter and the description of the close collisions with a straight line trajectory is of no crucial importance. For all the other cases, the application of the Anderson theory is very questionable due to the major role played by the impact parameters cutoff in the electronic clouds overlap region for the two colliding partners. This is, of course, the case of the diatom-atom collisions [7] but also the same as most of the diatom-diatom collisions for high rotational quantum numbers [8].

Many refinements to the Anderson theory have been introduced by Herman and Jarecki [9-11] concerning the widths and the shifts of vibration-rotation absorption lines induced by the pressure of rare gases. These refinements consist in modifying the trajectory model in favour of more realistic representation of the close collisions and by including the vibrational and rotational phase shift terms contributions up to infinite order. Murphy and

(*) Equipe de recherche associée au C.N.R.S.

Boggs [12] have also improved the Anderson second order limited treatment by including some of the higher order terms through an exponential form of the collision cross section. This avoids the use of a cutoff procedure but this theory maintains an unrealistic trajectory model for the shortest approach and neglects elastic broadening effects.

Finally, an infinite order semiclassical theory for spectral line broadening in molecules was recently proposed by Smith, Giraud and Cooper [13]. This theory uses curved classical trajectories determined by the isotropic part of the intermolecular potential and leads to a good agreement with close coupling calculations and with experiments [13, 14]. The extension of this theory to the rare gas pressure shifting of the diatomic molecules vibration-rotation lines was made by Boulet and Robert [15]. Nevertheless this semi-numerical treatment is hardly applicable to the diatom-diatom collisions and, of course, to molecular systems with a larger number of atoms due to the formidable computational task required. *A fortiori*, the same remark holds for all the fully quantum methods of calculation (i.e. close coupling) for the molecular collision cross sections, even when *dimensionality reducing* schemes are used such as in the coupled states approximation [16] or in the effective potential approximation [17]. This explains the persistent success of the various improved Anderson theories mentioned above [10, 12] specially for large molecules of astrophysical interest [18-23].

The aim of this paper is to introduce further improvements mainly concerning the close collisions contributions while still keeping an *analytical* treatment in order to extend the formalism proposed for isolated lines to more involved situations such as, for instance, the overlapped lines. Indeed, in the case of the isotropic Raman Q branches and of microwave bands of almost all the molecules, the lines begin to overlap each other even at moderate densities (several amagat units). Consequently significant deviations appear between the experimental data and the calculations issued from the isolated lines theories [24-28], so further theoretical investigations are required.

2. **General formulation.** — According to the general impact theory developed by Fano [29] and extended by Ben Reuven [30], the contour of the spectrum is determined by the following equation expressed in terms of reduced matrix elements

$$I(\omega) = -\pi^{-1} n_a \operatorname{Im} \frac{1}{2J+1} \sum_{\substack{v_i, j_i, j_i' \\ v_f, j_f, j_f'}} \langle v_i j_i \mid \rho_a \mid v_i j_i \rangle \langle v_i j_i \parallel X^{(J)} \parallel v_f j_f \rangle \times$$
$$\times \langle\langle v_f j_f v_i j_i J \mid (\omega - L_a - \Lambda)^{-1} \mid v_f' j_f' v_i' j_i' J \rangle\rangle \langle v_f' j_f' \parallel X^{(J)} \parallel v_i' j_i' \rangle . \quad (1)$$

In this equation L_a is the Liouville operator characterizing the unperturbed optically active molecule ($L_a \equiv [H_a \cdot]$), ρ_a is the corresponding density operator, n_a is the numerical density of the active molecules and $X^{(J)}$ the coupling tensor of J order between the molecules and the external field ($J = 0$ for the isotropic Raman diffusion, $J = 1$ for the electric dipolar absorption and $J = 2$ for the anisotropic Raman diffusion). The matrix element of the relaxation operator in the vibration-rotation states of the free optically active molecule may be expressed in terms of the $\hat{S}$ matrix in the Liouville space [30, 31].

$$\langle\langle v_f' j_f' v_i' j_i' J \mid \Lambda \mid v_f j_f v_i j_i J \rangle\rangle \equiv \Lambda_{f'i',fi} = -i \frac{n_b}{2\pi c} \times$$
$$\times \langle \{ \delta_{v_f' v_f} \delta_{j_f' j_f} \delta_{v_i' v_i} \delta_{j_i' j_i} - \langle\langle v_f' j_f' v_i' j_i' J \mid \hat{S} \mid v_f j_f v_i j_i J \rangle\rangle \} \rangle_{b,v,2} \quad (2)$$

where

$$\langle \hat{S} \rangle_2 = \sum_{\substack{v_2 j_2 \\ v_2' j_2'}} \langle\langle v_2' j_2' v_2' j_2' 0 \mid \hat{S} \mid v_2 j_2 v_2 j_2 0 \rangle\rangle \langle v_2 j_2 \mid \rho_b \mid v_2 j_2 \rangle$$

and

$$\mid v_f j_f v_i j_i J \rangle\rangle = \sum_{m_i, m_f} (-1)^{m_i} C(j_f j_i J ; m_f, -m_i, M) \mid v_f j_f m_f \rangle \mid v_i j_i m_i \rangle^+ .$$

In eq. (2) ρ_b and n_b are the density operator and the numerical density of the perturbers, $C(j_f j_i J ; m_f, -m_i, M)$ is the Clebsh-Gordan coefficient [32] and the symbol $\langle \ldots \rangle_{b,v,2}$ means an ensemble average over the impact parameter, the relative velocity and over the quantum states of the perturbers.

Moreover the $\hat{S}$ operator is defined through

$$\hat{S} = \theta \exp \left\{ -i\hbar^{-1} \int_{-\infty}^{+\infty} \mathrm{d}t \hat{V}(t) \right\}, \quad \hat{V}(t) = \mathrm{e}^{i\hbar^{-1}(\hat{H}_a + \hat{H}_b)t} \hat{V} \mathrm{e}^{-i\hbar^{-1}(\hat{H}_a + \hat{H}_b)t} \quad (3)$$

where the symbol θ means the time ordering operator, H_a and H_b are the Hamiltonians of the optically active molecule and of the perturber and V the coupling operator between these two molecules. The non-diagonal terms of the relaxation matrix with respect to the vibrational and rotational quantum numbers of the optically active molecule are called the *cross correlations terms* [30], they describe the non-additivity effects resulting from the lines overlap [30, 33, 34]. The influence of such terms on the resulting spectrum will be examined in a further paper but, for the presently studied isolated lines, these cross correlations contributions must be disregarded. In this case, the half-width at half-intensity γ_{fi} and the shift δ_{fi} of the Lorentzian line $i \rightarrow f$ is given by :

$$\Lambda_{fi,fi} = \delta_{fi} - i\gamma_{fi} . \tag{4}$$

From eqs. (2) to (4) it is seen that the analytical calculation of the γ_{fi} and δ_{fi} line parameters requires knowledge of the following matrix elements of the Liouville $\hat{S}$ matrix

$$\ll v_f j_f v_i j_i J ; v_2' j_2' v_2' j_2' 0 \mid \hat{S} \mid v_f j_f v_i j_i J ; v_2 j_2 v_2 j_2 0 \gg \cong$$

$$\cong \ll v_f j_f v_2' j_2' v_i j_i v_2' j_2' J \mid \hat{S} \mid v_f j_f v_2 j_2 v_i j_i v_2 j_2 J \gg \equiv \ll \text{f2'i2'} \mid \hat{S} \mid \text{f2i2} \gg \tag{5}$$

with (cf. eq. (2))

$$\mid v_f j_f v_2 j_2 v_i j_i v_2 j_2 J \gg =$$

$$= \sum_{m_i, m_f, m_2} (-1)^{m_i} C(j_f j_i J ; m_f, -m_i, M) (-1)^{j_2} \frac{1}{\sqrt{2j_2 + 1}} \mid v_f j_f m_f v_2 j_2 m_2 \rangle \mid v_i j_i m_i v_2 j_2 m_2 \rangle^+ .$$

The approximation made in the above equation (i.e. the decoupling of the angular momenta tied to the active molecule and to the perturber) must be connected to the *classical path* assumption. Indeed in this case the total angular momentum is much larger than internal angular momenta. So, the orbital angular momentum may be considered sufficient to describe the rotational part of the relative motion (the impact parameter approach developed in section 3) and the decoupling mentioned just above may be stated.

The $\ll$ f2'i2' $\mid \hat{S} \mid$ f2i2 $\gg$ matrix elements will be now expanded through the linked cluster theorem [35, 36]. These matrix elements are then expressed as a product of an exponential of the *connected* $\hat{V}$ matrix elements (noted by the (C) index) and of the *linked* elements (noted by the (L) index). For the isolated lines, these linked terms result only from the non-diagonality of $\hat{S}$ with respect to the states of the perturber. When limiting the expansion to the second order diagrams, we obtain

$$\ll \text{f2'i2'} \mid \hat{S} \mid \text{f2i2} \gg = \left[\delta_{2'2} - i\hbar^{-1} \int_{-\infty}^{+\infty} dt \ll \text{f2'i2'} \mid \hat{V}(t) \mid \text{f2i2} \gg_{(L)} - \right.$$

$$\left. - \hbar^{-2} \int_{-\infty}^{+\infty} dt \int_{-\infty}^{t} dt' \ll \text{f2'i2'} \mid \hat{V}(t)\, \hat{V}(t') \mid \text{f2i2} \gg_{(L)} \right] \tag{6}$$

$$\exp\left[- i\hbar^{-1} \int_{-\infty}^{+\infty} dt \ll \text{f2i2} \mid \hat{V}(t) \mid \text{f2i2} \gg_{(C)} \right] = [\delta_{2'2} - S_2^{(L)}]\ e^{-iS_1^{(C)} - S_2^{(C)}} .$$

The first order contribution ($S_1^{(C)}$; note that $S_1^{(L)} = 0$) and the second order contributions ($S_2^{(C)}$ and $S_2^{(L)}$) are defined through the following equations

$$S_1^{(C)} = S_{1,f2} - S_{1,i2}$$

$$S_2^{(C)} = S_{2,f2} + S_{2,i2} + S_{2,f2i2}^{(C)} + i[S'_{2,f2} - S'_{2,i2}] \equiv S_2 + iS'_2 \tag{7}$$

with

$$S_{2,f2i2}^{(C)} = \sum_{v_2', j_2'} S_{2,f2'i2'}\, \delta_{v_2' v_2}\, \delta_{j_2' j_2}$$

$$S_2^{(L)} = S_{2,f2i2}^{(L)} = \sum_{v_2' j_2'} S_{2,f2'i2'}(1 - \delta_{v_2' v_2}\, \delta_{j_2' j_2})$$

where

$$S_{1,i2} = \hbar^{-1} \int_{-\infty}^{+\infty} dt \langle v_i v_2 \mid V_{ISO}[r(t)] \mid v_i v_2 \rangle \tag{8}$$

$$S_{2,i2} = \frac{\hbar^{-2}}{2} \sum_{v_i', v_2'} \left| \int_{-\infty}^{+\infty} dt\, e^{i\omega_{v_i v_2, v_i' v_2'} t} \langle v_i v_2 \mid V_{ISO}[r(t)] \mid v_i' v_2' \rangle \right|^2 (1 - \delta_{v_i v_i'}\, \delta_{v_2 v_2'}) + \frac{\hbar^{-2}}{2(2j_i + 1)(2j_2 + 1)} \times$$

$$\times \sum_{\substack{v_i', j_i', m_i' \\ v_2', j_2', m_2' \\ m_i, m_2}} \left| \int_{-\infty}^{+\infty} dt\, e^{i\omega_{v_i j_i v_2 j_2, v_i' j_i' v_2' j_2' t}} \langle v_i j_i m_i v_2 j_2 m_2 \mid V_{ANISO}[r(t)] \mid v_i' j_i' m_i' v_2' j_2' m_2' \rangle \right|^2 \tag{9}$$

$$S'_{2,i2} = \frac{\hbar^{-2}}{2\pi} \sum_{v'_i, v'_2} \text{P.P.} \int_{-\infty}^{+\infty} \frac{d\omega}{\omega_{v_i v_2, v'_i v'_2} - \omega} \left| \int_{-\infty}^{+\infty} dt\, e^{i\omega t} \langle v_i\, v_2 \mid V_{ISO}[r(t)] \mid v'_i\, v'_2 \rangle \right|^2 +$$

$$+ \frac{\hbar^{-2}}{(2j_i + 1)(2j_2 + 1)} \frac{1}{2\pi} \sum_{\substack{v'_i, j'_i, m'_i \\ v'_2, j'_2, m'_2 \\ m_i, m_2}} \text{P.P.} \int_{-\infty}^{+\infty} \frac{d\omega}{\omega_{v_i j_i v_2 j_2, v'_i j'_i v'_2 j'_2} - \omega}$$

$$\times \left| \int_{-\infty}^{+\infty} dt\, e^{i\omega t} \langle v_i\, j_i\, m_i\, v_2\, j_2\, m_2 \mid V_{ANISO}[r(t)] \mid v'_i\, j'_i\, m'_i\, v'_2\, j'_2\, m'_2 \rangle \right|^2 \qquad (10)$$

$$S_{2,f2'i2'} = -\hbar^{-2} \int_{-\infty}^{+\infty} dt\, e^{i\omega_{v'_2, v_2} t} \langle v_f\, v'_2 \mid V_{ISO}[r(t)] \mid v_f\, v_2 \rangle \int_{-\infty}^{+\infty} dt'\, e^{i\omega_{v_2, v'_2} t'} \langle v_i\, v_2 \mid V_{ISO}[r(t')] \mid v_i\, v'_2 \rangle \times$$

$$\times (1 - \delta_{v'_2 v_2}) - \frac{\hbar^{-2}}{(2j_i + 1)(2j_2 + 1)} \sum_{\substack{m_f, m'_f, m_i, m'_i \\ m_2, m'_2}} C(j_f\, Jj_i\, ; m_f, M, m_i)\, C(j_f\, Jj_i\, ; m'_f, M, m'_i)$$

$$\times \int_{-\infty}^{+\infty} dt\, e^{i\omega_{v'_2 j'_2, v_2 j_2} t} \langle v_f\, j_f\, m'_f\, v'_2\, j'_2\, m'_2 \mid V_{ANISO}[r(t)] \mid v_f\, j_f\, m_f\, v_2\, j_2\, m_2 \rangle$$

$$\times \int_{-\infty}^{+\infty} dt'\, e^{i\omega_{v_2 j_2, v'_2 j'_2} t'} \langle v_i\, j_i\, m_i\, v_2\, j_2\, m_2 \mid V_{ANISO}[r(t')] \mid v_i\, j_i\, m'_i\, v'_2\, j'_2\, m'_2 \rangle . \qquad (11)$$

In these equations V_{ANISO} means the anisotropic part of the intermolecular potential, P.P. the Cauchy principal part, and the expressions for $S_{1,f2}$, $S_{2,f2}$ and $S'_{2,f2}$ will be respectively deduced from eqs. (8), (9) and (10), by only changing the subscript i to f.

Some additional remarks must be stated as far as the above relations are concerned. First, the inelastic vibrational contributions ($v' \neq v$) are always negligible for the cases considered here. Secondly, the pure vibrational dephasing contribution corresponding to the diagonal terms in the vibrational states of the isotropic part of the potential V (called V_{ISO}) is rigorously taken into account up to the infinite order through the S_1 contribution if the vibration-rotation coupling is disregarded (cf. eqs. (6), (7) and (8)). Also, the imaginary part of the second order contribution (cf. eqs. (7) and (10)) results from the noncommutative character of V in the interaction representation (cf. eq. (3)) at two different instants [37, 6, 15].

Starting from eqs. (2) to (11) the resulting expressions for the half-width at half-intensity γ_{fi} and for the line shift δ_{fi} (or for the corresponding collision cross sections σ_{fi} and σ'_{fi}) are thus given by

$$\gamma_{fi}\,(\text{cm}^{-1}) \equiv \frac{n_b}{2\pi c} v\sigma_{fi} = \frac{n_b}{2\pi c} \sum_{v_2, j_2} \rho_{v_2, j_2} \times$$

$$\times \int_0^\infty v f(v)\, dv \int_0^\infty 2\pi b\, db \{ 1 - [1 - S^{(L)}_{2,f2i2}]\, e^{-(S_{2,f2} + S_{2,i2} + S^{(C)}_{2,f2i2})} \cos [(S_{1,f2} + S'_{2,f2}) - (S_{1,i2} + S'_{2,i2})] \}$$

$$\delta_{fi}\,(\text{cm}^{-1}) \equiv \frac{n_b}{2\pi c} v\sigma'_{fi} = \frac{n_b}{2\pi c} \sum_{v_2, j_2} \rho_{v_2, j_2} \times \qquad (12)$$

$$\times \int_0^\infty v f(v)\, dv \int_0^\infty 2\pi b\, db \{ [1 - S^{(L)}_{2,f2i2}]\, e^{-(S_{2,f2} + S_{2,i2} + S^{(C)}_{2,f2i2})} \sin [(S_{1,f2} + S'_{2,f2}) - (S_{1,i2} + S'_{2,i2})] \} . \qquad (13)$$

The eqs. (12) and (13) are similar to those recently derived by Mehrotra and Boggs [38] but they include the additional contribution coming from the rotational dephasing effects through the $S^{(C)}_{2,f2i2}$ and $S^{(L)}_{2,f2i2}$ terms (cf. eqs. (7) and (11)). These elastic broadening effects are of importance for all the cases studied here (cf. sect. 5 and Figs. 9). We mention that such an approach avoids the use of any questionable cutoff procedure due to the partial resummation of the V-infinite series through the connected terms.

When neglecting some of the contributions coming from the orientational terms of order higher than two as done in eqs. (12) and (13), the main problem arising in an effective calculation of the γ_{fi} and δ_{fi} parameters is connected with the trajectory description, especially for the close collisions.

3. **Kinematical model for the binary collisions.** — Almost all line width calculations neglect the influence of the isotropic interactions V_{ISO} on classical tra-

jectories [12, 38], the usual model being a straight line trajectory described with constant velocity [1-3]. A first analytical model was proposed by Tipping and Herman [9] including the influence of V_{ISO} in the energy conservation equation. Nevertheless this model neglects the influence of the force $\mathbf{F}_{ISO}$ (derived from the isotropic potential V_{ISO}) in the equation of motion around the distance of closest approach r_c. Consequently, this trajectory description is not valid for hard collisions such as $b < r_0$ where r_0 is the r_c value for a head-on collision.

Recently L. Bonamy and the present authors [39] included the above-mentioned influence of $\mathbf{F}_{ISO}$ in the $\mathbf{r}(t)$ equation

$$\mathbf{r}(t) \cong \mathbf{r}_c + \mathbf{v}_c\, t + \frac{\mathbf{F}_c}{m}\frac{t^2}{2} \qquad (14)$$

where $\mathbf{v}_c$ is the relative velocity at the closest approach and $\mathbf{F}_c$ is defined through

$$\mathbf{F}_c = -\left(\frac{\partial V_{ISO}}{\partial r}\right)_{r=r_c}\frac{\mathbf{r}_c}{r_c} = \frac{24\,\varepsilon}{\sigma}\left[2\left(\frac{\sigma}{r_c}\right)^{13} - \left(\frac{\sigma}{r_c}\right)^{7}\right]\frac{\mathbf{r}_c}{r_c} \qquad (15)$$

ε and σ being the usual Lennard-Jones constants.

The $r(t)$ modulus is then given by

$$r(t) = [r_c^2 + v_c'^2\, t^2]^{1/2} \qquad (16)$$

where the *apparent* relative velocity v_c' is defined through

$$v_c'^2 = v_c^2 + \frac{\mathbf{F}_c \cdot \mathbf{r}_c}{m}. \qquad (17)$$

Taking into account the conservation of the angular momentum ($v_c\, r_c = vb$) and of the energy

$$(1/2\, mv^2 = 1/2\, mv_c^2 + 4\,\varepsilon[(\sigma/r_c)^{12} - (\sigma/r_c)^6]),$$

v_c' is given by

$$v_c' = v\left\{1 + \frac{8\,\varepsilon}{mv^2}\left[5\left(\frac{\sigma}{r_c}\right)^{12} - 2\left(\frac{\sigma}{r_c}\right)^{6}\right]\right\}^{1/2}. \qquad (18)$$

The variation of r_c/σ issued from these conservation equations as a function of b/σ (eq. (18)) is presented on figure 1 for various values of the reduced physical parameter $E^* = mv^2/2\,\varepsilon$. Figure 1 exhibits the existence of orbiting collisions which appear at sufficiently low values of v. In fact for the current physical situations the considered mean kinetic energy is higher than the ε values and the orbiting collisions are not efficient. Nevertheless it should be mentioned that for sufficiently low temperatures ($T \lesssim \varepsilon/k$) the Maxwellian distribution of velocities provides a noticeable fraction of weak relative velocities which gives rise to orbiting collisions. The duration of these collisions increases the correlation time considerably and a strong increase of the line widths has to be expected in this case. Such a temperature behaviour was recently observed [40] in the anisotropic Raman spectrum of pure H_2, D_2 and HD for $T < 50$ K and might be explained by the above considerations.

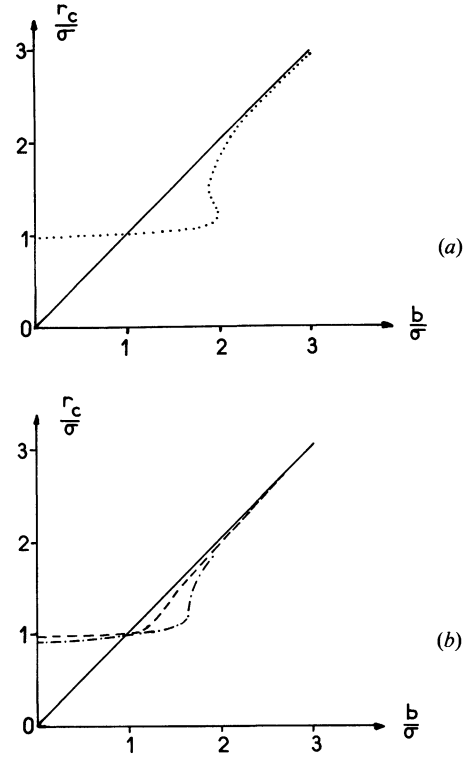

Fig. 1. — The influence of curved trajectories on the reduced distance of closest approach r_c/σ for various values of the reduced kinetic energy $E^* = mv^2/2\,\varepsilon$. 1*a*. — this case ($E^* = 0.5$) corresponds to a type of collisions in which *orbiting* takes places. 1*b*. — The two curves (.—.—. $E^* = 1$; — — — $E^* = 4$) correspond to *open* trajectories for the whole range of b/σ values.

The variation of v_c'/v *versus* b/σ plotted on figure 2 shows a marked deviation from unity for low b values ($b \lesssim \sigma$) especially for low reduced kinetic energies.

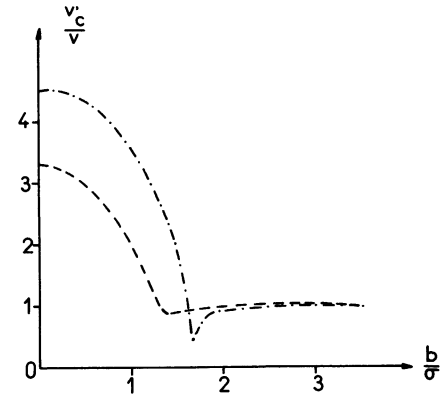

Fig. 2. — The *apparent* reduced velocity $\frac{v_c'}{v}$ at the distance of closest approach in our parabolic trajectory model (.—.—. $E^* = 1$; — — — $E^* = 4$).

In the approximation of eq. (16), the real curved trajectory was replaced by an equivalent straight path. Another curved trajectory model is now proposed which includes the $\mathbf{F}_c$ influence in the $\psi(t)$ collision angle (cf. Fig. 3) at the second order in t, as was done for $\mathbf{r}(t)$ in eq. (14), i.e.

$$\sin \psi(t) \cong \frac{v_c\, t}{[r_c^2 + v_c'^2\, t^2]^{1/2}}\,;$$
$$\cos \psi(t) \cong \frac{r_c + \dfrac{|\mathbf{F}_c|}{m}\dfrac{t^2}{2}}{[r_c^2 + v_c'^2\, t^2]^{1/2}}\,. \qquad (19)$$

(Note that for the homogeneity of the present development the condition $\cos^2 \psi(t) = 1 - \sin^2 \psi(t)$ has to be respected.)

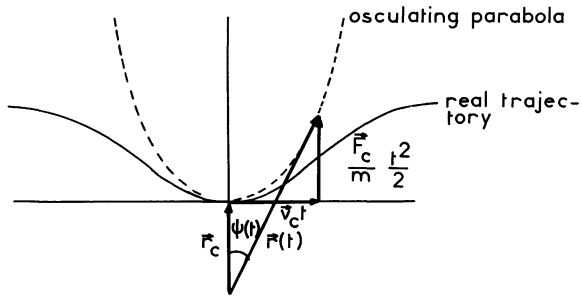

Fig. 3. — Geometry of the collision (in the particular type of collision represented here, the repulsive forces are most important).

A similar parabolic trajectory was introduced by Gersten [41] in the collision-induced light scattering and was very recently discussed by Berard et Lallemand [42] in a systematic analysis of the potential correlation function calculation. These authors showed that it is compulsory to use trajectories with the true relative velocity at the closest distance of approach as is the case in our model.

It may be noticed that for very distant collisions ($b \gg \sigma$) this model tends to be the usual straight path trajectory, the influence of the isotropic potential being negligible. In the opposite situation ($b \lesssim \sigma$) such an influence is crucial. In particular, for the head-on collisions the *apparent* relative velocity is not zero (cf. Fig. 2) as in the Tipping and Herman model [9] avoiding any unphysically behaviour for all the hard collisions. In this case ($b = 0$) the r_c and v_c' parameters are given by

$$r_0 = \sigma\left[\frac{2}{1 + \sqrt{1 + mv^2/2\,\varepsilon}}\right]^{1/6};$$
$$v'_{c_0} = v\left\{6\left[1 + \frac{2\,\varepsilon}{mv^2}(1 + \sqrt{1 + mv^2/2\,\varepsilon})\right]\right\}^{1/2}. \qquad (20)$$

Due to the role played by the r_c parameter in the above trajectory model it is more convenient to replace the average over the impact parameter b by the corresponding average over this parameter as follows

$$\int_0^\infty 2\pi b\, db \to \int_{r_0}^\infty 2\pi r_c\, dr_c \left(\frac{v_c'}{v}\right)^2. \qquad (21)$$

The various S_1 and S_2 terms appearing in eqs. (12) and (13) are now functions of r_c and v_c', the dependence of v_c' on r_c and v being given by eq. (18).

4. **Test of the present semiclassical model.** — The semiclassical theory of the width and the shift of the lines developed in sections 2 and 3 can be now applied to the pressure broadening by Argon of HCl pure rotational lines. This is a particularly valuable test for our present model of calculation for several reasons. First, Neilsen and Gordon [43] have performed a very accurate numerical solution of the Schrödinger equation using classical curved trajectories for the translational motion and second, Smith, Giraud and Cooper [13] have also tested their approximate infinite order theory for the same physical situation as in ref. [43]. Moreover this theory was successfully compared to close coupling calculations for CO-He cross sections. Therefore, in order to have a physically meaningful comparison, it is particularly interesting to calculate also the rotational line width for HCl-A using the theoretical framework developed above and using this potential labelled N.G.52 [43]. Also it should be mentioned that as far as diatom-atom collisions are concerned the role played by the close collisions is drastic making this test very severe.

In fact our calculations were performed by using the same potential as that of Smith *et al.* [13]. It differs from the potential of Neilsen and Gordon due to the substitution by a r^{-12} analytical dependence of the repulsive terms to the exponential form

$$V(r, \theta) \equiv V_0(r) + V_1(r, \theta) + V_2(r, \theta) = 4\,\varepsilon\left[\left\{\left(\frac{\sigma}{r}\right)^{12} - \left(\frac{\sigma}{r}\right)^{6}\right\} + \left\{R_1\left(\frac{\sigma}{r}\right)^{12} - A_1\left(\frac{\sigma}{r}\right)^{7}\right\} P_1(\cos\theta) + \left\{R_2\left(\frac{\sigma}{r}\right)^{12} - A_2\left(\frac{\sigma}{r}\right)^{6}\right\} P_2(\cos\theta)\right]. \qquad (22)$$

The values of the various parameters appearing in this equation are (cf. refs. [13] and [43]) $\varepsilon = 202$ K, $\sigma = 3.37$ Å, $R_1 = 0.37$, $R_2 = 0.65$, $A_1 = 0.33$, $A_2 = 0.14$. As for the Lennard-Jones parameters ε and σ which are not explicitely reported in ref. [13], their numerical values were obtained by numerically fitting the Neilsen and Gordon isotropic potential by a least-squares procedure.

Following eq. (12), the calculation of the half-width γ_{fi} for the pure rotational lines requires the specification (cf. eq. (7)) of the $S_2^{(C)}$ and $S_2^{(L)}$ terms (the $S_1^{(C)}$ terms obviously cancel out in the far infrared region since $v_i \equiv v_f$ and the S_2' contribution must be disregarded in the present text since they result from the non-commutative character of the intermolecular potential which was neglected in ref. [13] and [43]). As an example, we present now the detailed calculation of the S_2 term

$$(S_2 = S_{2,f2} + S_{2,i2} + S^{(C)}_{2,f2i2}) ;$$

cf. (eqs. (7) (9) and (11)) for the particular case of the $P_1(\cos\theta)$ contribution appearing in eq. (22). The kinematical model used for the binary collisions is the same as in section 3.

The expression of this potential contribution in the collision frame [44] is

$$V_1(r, \psi) = 4\,\varepsilon \left\{R_1\left(\frac{\sigma}{r}\right)^{12} - A_1\left(\frac{\sigma}{r}\right)^{7}\right\} \times \times [F \cos\psi - F' \sin\psi] \quad (23)$$

with

$$F = -\frac{4\pi}{\sqrt{3}} Y_0^1(1)\, Y_0^0(2)$$

$$F' = i\frac{4}{\sqrt{6}}[Y_1^1(1)\, Y_0^0(2) + Y_{-1}^1(1)\, Y_0^0(2)] . \quad (24)$$

The matrix element between the eigenstates i and i′ of the unperturbed Hamiltonian, appearing in eq. (9), is

$$P_{ii'} = \hbar^{-1} \int_{-\infty}^{+\infty} dt\, e^{i\omega_{ii'}t} \langle i \mid V_1[r(t), \psi(t)] \mid i' \rangle$$
$$= 4\,\varepsilon\hbar^{-1}[(R_1 \hat{G}_{12} - A_1 \hat{G}_7) F + (R_1 \hat{G}'_{12} - A_1 \hat{G}'_7) F'] \quad (25)$$

where

$$\hat{G}_l \text{ (or } \hat{G}'_l) = \int_{-\infty}^{+\infty} dt\, e^{i\omega_{ii'}t} \frac{\sigma^l}{r^l} \times \cos\psi(t) \text{ (or } \sin\psi(t)) . \quad (26)$$

By putting

$$k = \frac{\omega_{ii'} r_c}{v'_c} \quad \text{and} \quad z = \frac{v'_c t}{r_c},$$

and by using the expressions of $\sin\psi(t)$ and $\cos\psi(t)$ of eq. (19), one obtains

$$\hat{G}_l = \frac{1}{v'_c}\left(\frac{\sigma}{r_c}\right)^l \int_{-\infty}^{+\infty} dz \frac{e^{ikz}}{(1+z^2)^{(l+1)/2}} + \frac{1}{2}\left(1 - \frac{v_c^2}{v_c'^2}\right) \int_{-\infty}^{+\infty} dz \frac{e^{ikz} z^2}{(1+z^2)^{(l+1)/2}} \quad (27)$$

$$\hat{G}'_l = \frac{1}{v'_c}\left(\frac{v_c}{v'_c}\right)\left(\frac{\sigma}{r_c}\right)^l \int_{-\infty}^{+\infty} dz \frac{e^{ikz} z}{(1+z^2)^{(l+1)/2}} . \quad (28)$$

The general expression for the integrals appearing in eqs. (27) and (28) is given in ref. [2]. So, we obtain the following differential cross section

$$^{1,0}S_2(r_c(b)) = \left(\frac{4\,\varepsilon\sigma}{\hbar v'_c}\right)^2 \left\{\frac{25\,\pi^2}{1\,536} A_1^2 \left(\frac{\sigma}{r_c}\right)^{12} \left(\sum_{j'_i} C_{j'_i}^{(1)\ 1,0} f_7^7(k) + \sum_{j''_f} C_{j''_f}^{(1)\ 1,0} f_7^7(k)\right) -$$
$$- \frac{160\,\pi}{2\,079} A_1 R_1 \left(\frac{\sigma}{r_c}\right)^{17} \left(\sum_{j'_i} C_{j'_i}^{(1)\ 1,0} f_7^{12}(k) + \sum_{j''_f} C_{j''_f}^{(1)\ 1,0} f_7^{12}(k)\right)$$
$$+ \frac{131\,072}{1\,440\,747} R_1^2 \left(\frac{\sigma}{r_c}\right)^{22} \left(\sum_{j'_i} C_{j'_i}^{(1)\ 1,0} f_{12}^{12}(k) + \sum_{j''_f} C_{j''_f}^{(1)\ 1,0} f_{12}^{12}(k)\right)\Bigg\} \quad (29)$$

with

$$C_{j_i}^{(n)} = |\, C(j_i\, n j_i' \,;\, 000)\,|^2\,, \qquad C_{j_f}^{(n)} = |\, C(j_f\, n j_f' \,;\, 000)\,|^2\,.$$

The left superscripts appearing in the resonance f-functions (i.e. 1, 0) are directly related to the orders of the spherical harmonics for the active molecule and the perturber respectively. The right symbols relate to the radial exponent of the potential term connected to the considered resonance function. Note that ${}^{1,0}S^{(L)}_{2,f2i2} = 0$ and ${}^{1,0}S_2 = {}^{1,0}S_{2,f} + {}^{1,0}S_{2,i}$ since ${}^{1,0}S^{(C)}_{2,f2i2} = 0$ (cf. eq. (7)).

A similar calculation for the $P_2(\cos\theta)$ contribution in eq. (22) leads to

$$\begin{aligned} {}^{2,0}S(r_c(b)) = \left[\frac{4\,\varepsilon\sigma}{\hbar v_c'}\right]^2 \Bigg\{ & \frac{21\,\pi^2}{2\,560} A_2^2 \left(\frac{\sigma}{r_c}\right)^{10} \left(\sum_{j_i} C_{j_i}^{(2)}\, {}^{2,0}f_6^6(k) + \sum_{j_f} C_{j_f}^{(2)}\, {}^{2,0}f_6^6(k) + D\right) \\ & - \frac{63\,\pi^2}{5\,120} A_2\, R_2 \left(\frac{\sigma}{r_c}\right)^{16} \left(\sum_{j_i} C_{j_i}^{(2)}\, {}^{2,0}f_6^{12}(k) + \sum_{j_f} C_{j_f}^{(2)}\, {}^{2,0}f_6^{12}(k) + D\right) \\ & + \frac{48\,951\,\pi^2}{10\,485\,760} R_2^2 \left(\frac{\sigma}{r_c}\right)^{22} \left(\sum_{j_i} C_{j_i}^{(2)}\, {}^{2,0}f_{12}^{12} + \sum_{j_f} C_{j_f}^{(2)}\, {}^{2,0}f_{12}^{12}(k) + D\right) \Bigg\} \end{aligned} \tag{30}$$

with

$$D = (-1)^{j_i + j_f}\, 2[(2j_i + 1)(2j_f + 1)\, C_{j_i}^{(2)}\, C_{j_f}^{(2)}]^{1/2}\, W(j_i\, j_f\, j_i\, j_f\,;\, 12)$$

where W is the Racah coefficient [2]. Note that ${}^{2,0}S^{(L)}_{2,f2i2} = 0$.

The expressions of the resonance functions appearing in eqs. (29) and (30) are given in Appendix A. Note that these f-functions differ from the resonance functions appearing in the previous theories (see for instance refs. [2, 3, 9 and 12]). Indeed their argument is now defined by the closest approach distance r_c and the *apparent* relative velocity v_c' (cf. eq. (18)) through $k = \dfrac{\omega_{i'}\, r_c}{v_c'}$, instead of the impact parameter b and the relative velocity v respectively. Moreover the parabolic trajectory model leads to an additional dependence of these functions on v_c/v_c' as evidenced in eq. (27) and in the expressions given in Appendix A

$$\frac{v_c}{v_c'} = \left\{\frac{1 - (8\,\varepsilon/mv^2)\,[(\sigma/r_c)^{12} - (\sigma/r_c)^6]}{1 + (8\,\varepsilon/mv^2)\,[5(\sigma/r_c)^{12} - 2(\sigma/r_c)^6]}\right\}^{1/2}. \tag{31}$$

Of course for distant collisions ($r_c \sim b \gg \sigma$) (cf. Fig. 1) one has $v_c' \sim v_c \sim v$ (see eqs. (17) and (18) and Fig. 2) and all the f-functions tend to be the corresponding Anderson resonance functions [2]. In order to illustrate the behaviour of these f-functions, we give on figures 4*a* and 4*b* the variation of ${}^{1,0}f_7^7(k)$ and ${}^{2,0}f_6^6(k)$ as a function of k. These figures exhibit

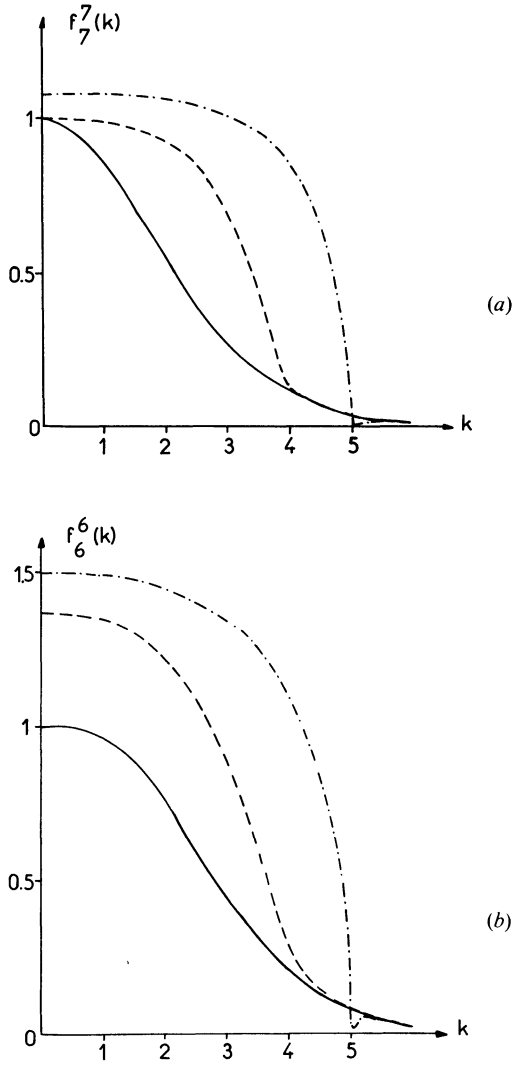

Fig. 4. — The resonance functions for two particular interactions obtained from the parabolic trajectory model are compared to the corresponding Anderson resonance functions (——— Anderson function, .—.—. $E^* = 1$, — — — $E^* = 4$). 4*a*. — Interaction in $\dfrac{P_1(\cos\theta)}{r^7}$ (cf. eq. (22)). 4*b*. — interaction in $\dfrac{P_2(\cos\theta)}{r^6}$ (cf. eq. (22)).

strong deviations from the Anderson functions mainly at low kinetic energy. The major effect of our kinematical model is to extend the k-region of resonance and thus to increase the number of efficient collisions for given b and v parameters.

The numerical calculations were performed using eq. (12) explicited through eqs. (29) and (30) for HCl-Ar with the conditions just outlined but by not averaging the cross section σ_{fi} over the relative velocity as was done in refs. [43] and [13]. We compare in table I the present results for various reduced kinetic energies $E^* = mv^2/2\,k$ with the corresponding values obtained from the Neilsen and Gordon [43] and Smith *et al.* [13] calculations. As it appears in table I our results agree within 10 % with the Smith *et al.* theory [13] reproducing moreover in a very consistent way the j and E^* dependences. The agreement with Neilsen and Gordon calculations [43] is less convincing, the j dependence being not so well reproduced. It must be recalled here that the numerical potential surfaces are not rigorously the same in the two cases (cf. *supra*) in opposition with the previous comparison and that the role of the anisotropic repulsive part of the potential is of crucial importance.

Table I. — *Unaveraged* HCl-Ar *cross sections for pure rotation transitions in* Å^2 *for various reduced kinetic energies* $E^* = mv^2/2\,k$.

	E^* = 808 K		E^* = 404 K		E^* = 398 K	
j_i	S-G-C([a])	This work	S-G-C([a])	This work	N-G([b])	This work
0	—	—	—	—	79.9	80.3
1	57.2	58.7	63.7	66.8	57.4	68.2
2	43.1	47.4	48.3	53.1	45.2	55.1
3	36.5	40.2	38.0	42.7	37.4	45.1
4	31.2	34.8	31.0	34.0	30.6	36.6
5	26.9	30.2	25.6	26.8	23.7	29.4

([a]) Calculated values from ref. [13].
([b]) Calculated values from ref. [43].

This test provides a useful confirmation of our theoretical approach and numerical calculations. We recall that the main advantage of such an approach lies in its analytical character (cf. eqs. (12), (13), (29) and 30)) and in the possibility to easily extend the domain of its applications to more involved situations (cf. following sections). In particular the diatom-diatom collisions cross sections calculations performed in the framework of the theories of refs. [43] and [13] will necessitate prohibitive computing times due to the thermal average over the rotational degrees of freedom of the perturber. This difficulty is removed in our theory and the remaining problem consists in deriving short ranged anisotropic potential surfaces, the long ranged part of the potential being correctly described by the electrostatic interactions. The first multipolar moments characterizing these interactions are generally well known for most of the studied molecules. Until now the anisotropic short ranged part of the diatom-diatom potential was calculated by *ab initio* methods only for very simple systems such as H_2-H_2 [45, 46]. Even the semi-empirical method proposed by Gordon and Kim [47] was applied only to the diatom-atom case [48-50]. Consequently strong interest lies in realistic model studies for describing these interactions. The next section is devoted to this particular aspect.

5. **Potential model for interactions between linear molecules.** — Several models have been proposed in order to get a realistic representation of the angle-dependent intermolecular potential. Among them, the most extensively studied are the so-called *atomic* [51-53], Kihara core [54] and overlap [55] models. A recent study of MacRury, Steele and Berne [52] showed that these three models were approximately equivalent for slightly non spherical molecules such as N_2 or CO_2. However, the *atomic* representation was the most widely used and gave a good fit to many experimental data. Concerning the molecules N_2 and CO_2, we will mention some experiments such as the second virial coefficients over a wide range of temperature [53, 56], the heat of sublimation [57], the crystal structure and the lattice frequencies of solids [58], the dimers configuration [59] and several equilibrium and dynamical properties of liquids [60]. The *atomic* model added to the electrostatic part of the potential constitutes a *sufficiently realistic representation* [52] of the interaction to warrant its use in the following (see, for instance, sect. 6).

Thus, the intermolecular potential V will be represented by the superposition of atom-atom interactions between the two colliding molecules (cf. Fig. 5) i.e. V_A, added to the electrostatic contribution V_E (here the quadrupolar interaction)

$$V = V_A + V_E = \sum_{i,j}\left(\frac{d_{ij}}{r^{12}_{1i,2j}} - \frac{e_{ij}}{r^{6}_{1i,2j}}\right) + V_{Q_1Q_2}\,. \quad (32)$$

In eq. (32) the indices i and j refer, respectively, to the ith atom of molecule 1 and the jth of molecule 2, $r_{1i,2j}$ is the distance between these two atoms, d_{ij} and e_{ij} are the atomic pair energy parameters and Q_1

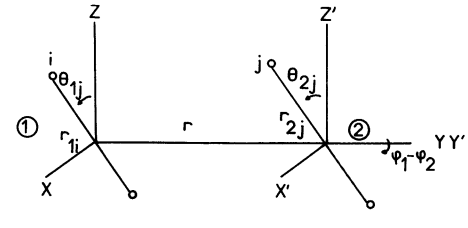

Fig. 5. — Orientational and radial coordinates for two interacting linear molecules.

and Q_2 are quadrupolar moments of each molecule. In the fixed frame of figure 5 it is possible to specify analytically the angular dependence of V_A (cf. eq. (32)) by expanding all the $r_{1i,2j}$ interatomic distances in terms of the intermolecular distance r, of the intramolecular distances r_{1i} and r_{2j} and of the spherical harmonics Y_l^m tied to each molecule [61, 52]. Thus for the intermolecular potential V we obtain :

$$V = \sum_{i,j} \sum_{q=0}^{n} \sum_{\substack{l_1=0 \\ l_2=0}}^{n} \sum_{m_1,m_2=-\inf(l_1,l_2)}^{+\inf(l_1,l_2)} \left\{ \frac{{}^{q}_{ij}D^{m_1 m_2}_{l_1 l_2}\, d_{ij}}{r^{12+q}} - \frac{{}^{q}_{ij}E^{m_1 m_2}_{l_1 l_2}\, e_{ij}}{r^{6+q}} \right\} Y^{m_1}_{l_1}(\theta_1, \varphi_1)\, Y^{m_2}_{l_2}(\theta_2, \varphi_2) +$$

$$+ \sum_{m_1',m_2'=-2}^{2} F^{m_1' m_2'}_{22} \frac{Q_1 Q_2}{r^5}\, Y^{m_1'}_{2}(\theta_1, \varphi_1)\, Y^{m_2'}_{2}(\theta_2, \varphi_2) \equiv 4\pi \sum_{l_1 l_2} \sum_{m=-\inf(l_1,l_2)}^{+\inf(l_1,l_2)} u_{l_1 l_2 m}(r)\, Y^{m}_{l_1}(\theta_1, \varphi_1)\, Y^{-m}_{l_2}(\theta_2, \varphi_2) . \quad (33)$$

Note that for the symmetric linear molecules considered here, only D and E coefficients with even $\{ l_1, l_2 \}$ are non-zero. The explicit calculations of these coefficients were performed up to and including fourth order ($q = 0$, 2 and 4). The corresponding expressions are given in Appendix B_1. Such a limited expansion, both in radial and angular coordinates (eq. (33)), may be tested for given quantum numbers $\{ l_1, l_2, m \}$ through the radial dependence of $u_{l_1 l_2 m}(r)$ by a comparison with the rigorous numerical calculations performed by MacRury *et al.* [52] including all r-orders. We chose the same values as those from the detailed study of ref. [52] for the physical parameters r_{1i}, r_{2j}, d_{ij}, e_{ij} and Q (cf. table II). The figures 6*a* to 6*c* justify the analytical expansion in the spherical harmonics limited to fourth order in a remarkable way. It is to be noted that the main contributions to the angle dependent part of the potential energy come from the u_{200}, u_{220} and in a less extent from the u_{221} components. The u_{222} term is very weak. Moreover the u_{400} coefficient has not been reported on figure 6 due to its negligible contribution (its values is 9 K for $r = \sigma$ and 1 K for the minimum of u_{000}) and this contribution will be disregarded in the following. These conclusions may be applied to CO_2 as it appears on figure 7.

In connection with the interest lying in the infrared and Raman spectral properties of CO, it is useful to get a realistic potential surface for this molecule. Although CO is not a symmetrical molecule, its dipole moment is very weak ($\mu = 0.11$ D) and its quadrupole moment is of the same order of magnitude as N_2 or CO_2 ($Q_{CO} = -2.23$ DÅ ; cf. table II). So, it is interesting to extend the atomic model to CO-CO, CO-N_2 and CO-CO_2 interactions since in a recent study of the second virial coefficients within a wide range of temperature, Oobatake and Ooi [53] determined the needed energy parameters in this model (cf. eq. (32)). Due to the non-symmetrical character of the CO molecule it is necessary to add the odd contributions to the tabulated terms of Appendix B_1. The ${}^{q}_{ij}D^{m_1 m_2}_{l_1 l_2}$ and ${}^{q}_{ij}E^{m_1 m_2}_{l_1 l_2}$ coefficients

Table II. — *Physical parameters characterizing the intermolecular potential for* N_2, CO_2 *and* CO *molecules.*

	$\varepsilon(k)$ (c)	σ (Å) (c)	d_{ij} (10^{-16} erg Å^{12}) (d)	e_{ij} (10^{-16} erg Å^{6}) (d)	$\lvert r_{1i} \rvert$ (or $\lvert r_{2j} \rvert$) (Å)	Q (10^{-26} e.s.u. cm^2)	B_0 (cm^{-1}) (f)
N_2 (a)	139	3.34	0.37×10^9	0.27×10^6	0.55	− 1.5	2.000 6
CO_2 (a)	519	2.98	0.35×10^9	0.50×10^6	1.19	− 3.9	0.389 5
CO (b)	$\varepsilon_{C-C} = 143$ $\varepsilon_{O-O} = 198$ $\varepsilon_{C-O} = 168$ (e)	$\sigma_{C-C} = 3.56$ $\sigma_{O-O} = 3.14$ $\sigma_{C-O} = 3.35$ (e)	$d_{C-C} = 0.82 \times 10^9$ $d_{O-O} = 0.25 \times 10^9$ $d_{C-O} = 0.46 \times 10^9$	$e_{C-C} = 0.40 \times 10^6$ $e_{O-O} = 0.26 \times 10^6$ $e_{C-O} = 0.33 \times 10^6$	$\lvert r_{1C} \rvert = 0.64$ $\lvert r_{1O} \rvert = 0.48$	− 2.23	1.922 6

(a) All values are taken from ref. [52]. Note that for the CO_2 molecule the exhaustive study of MacRury *et al.* [52] shows that only a very little change appears when a diatomic model rather than a triatomic model is used. Consequently we have retained here their recommanded diatomic (12,6) model.

(b) The here considered values for d_{ij} and e_{ij} (or ε and σ) have been obtained by Obatake and Ooi [53] from second virial coefficients measurements. Among the various possible choices for these parameters proposed by these authors we have selected those leading to the best fit with the isotropic intermolecular potential given in ref. [61] ($\varepsilon = 100.2$ K, $\sigma = 3.763$ Å for the molecular Lennard-Jones parameters).

(c) *Atomic* Lennard-Jones parameters characterizing the atom-atom interactions in the present considered model.

(d) Calculated values deduced from the two first columns.

(e) These values are obtained from the usual combination rules.

(f) Rotational constants taken from G. Herzberg, *Molecular Spectra and Molecular Structure* (Van Nostrand, Princeton, New Jersey) 1961.

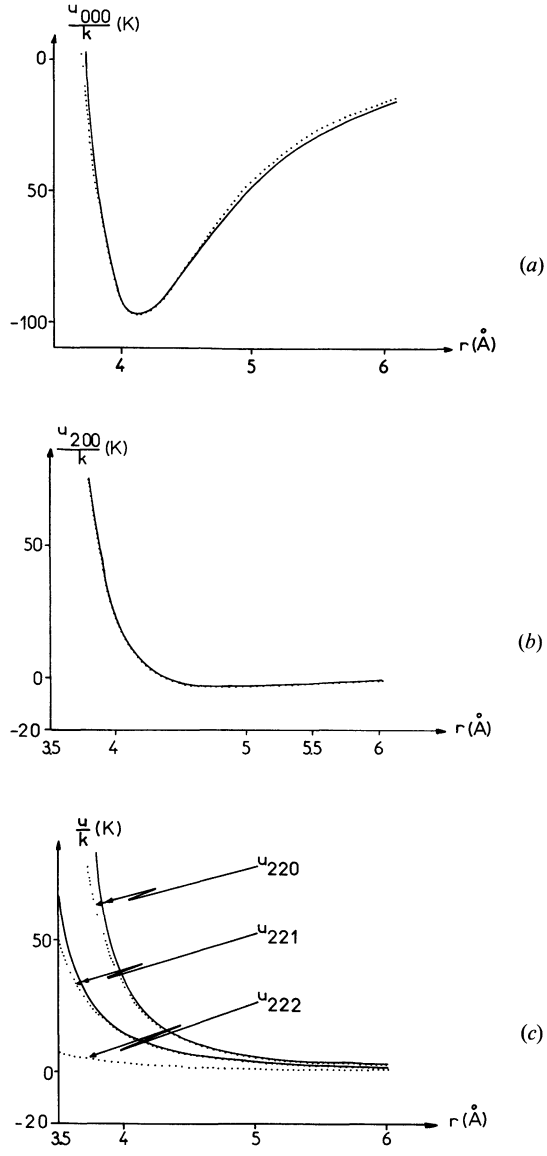

Fig. 6. — Coefficients $u_{l_1 l_2 m}(r)$ in the spherical harmonic expansion of the interaction energy between two N_2 molecules. (... calculated from eq. (33), analytical expressions of Appendix B_1 and the numerical values given in table II ; ——— numerical computation of Mac Rury *et al.* [52] including all r-orders.) 6*a*. — Isotropic part coefficient $u_{000}(r)$; 6*b*. — Anisotropic part coefficient $u_{200}(r)$; 6*c*. — Anisotropic part coefficient $u_{22m}(r)$ taking into account the quadrupolar contribution.

for $q = 1$, 2 and 3 with odd l_1 or l_2 indices derived in a previous work of the present authors [63] were reported in Appendix B_2. A study of the $u_{l_1 l_2}(r)$ corresponding coefficients (cf. Appendix B_2) defined above (cf. eq. (33)) shows (Fig. 8*a*) that the very predominant contributions come from the u_{100}, u_{200}, u_{110}, u_{120}, u_{210} and mainly from u_{220} if moreover we take into account its resonance properties in the collisional mechanisms (cf. sect. 6). In the following applications the u_{400} component will be neglected due to its very small contributions (only several K units for $r \gtrsim \sigma$). Moreover curves of interaction

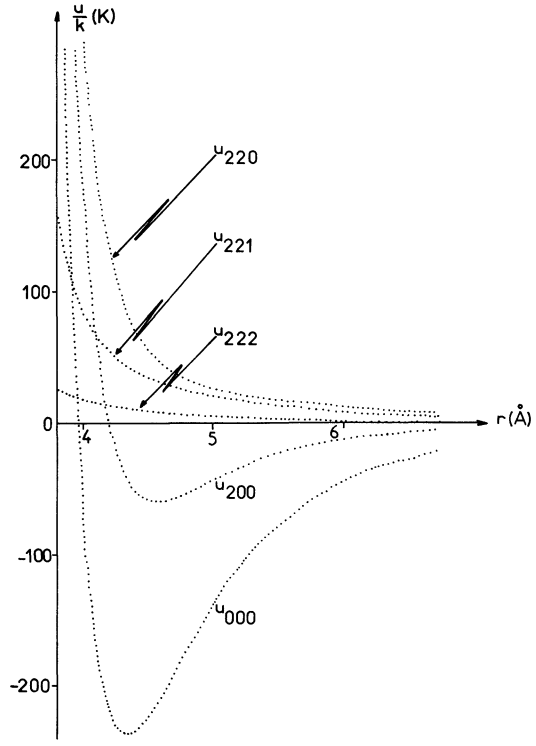

Fig. 7. — Coefficients $u_{l_1 l_1 m}(r)$ for the interaction between two CO_2 molecules calculated from eq. (33), Appendix B_1 and numerical values given in table II.

energy for pairs of CO molecules with fixed orientations are shown on figure 8*b*. The comparison of figure 8*b* with the corresponding figures of ref. [52] for N_2 and CO_2 pairs also shows a similar behaviour.

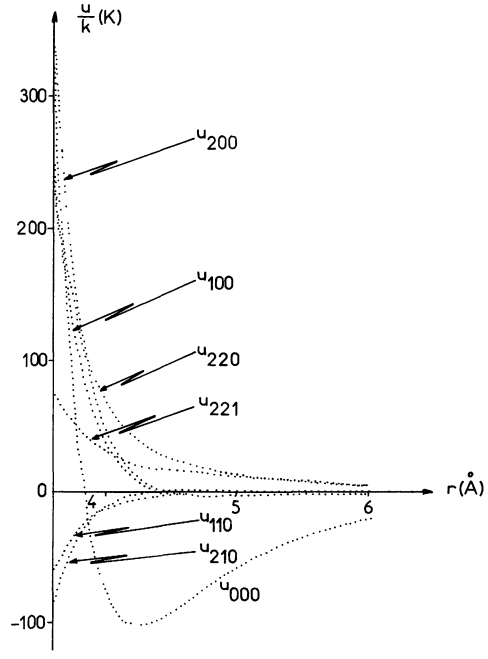

Fig. 8*a*. — Coefficients $u_{l_1 l_2 m}(r)$ for the interaction between two CO molecules calculated from eq. (33), Appendix B and numerical values given in table II. The u_{111}, u_{211}, u_{121} and u_{400} contributions have not been reported because of their small magnitude. Note moreover that here $u_{12m} = -u_{21m}$.

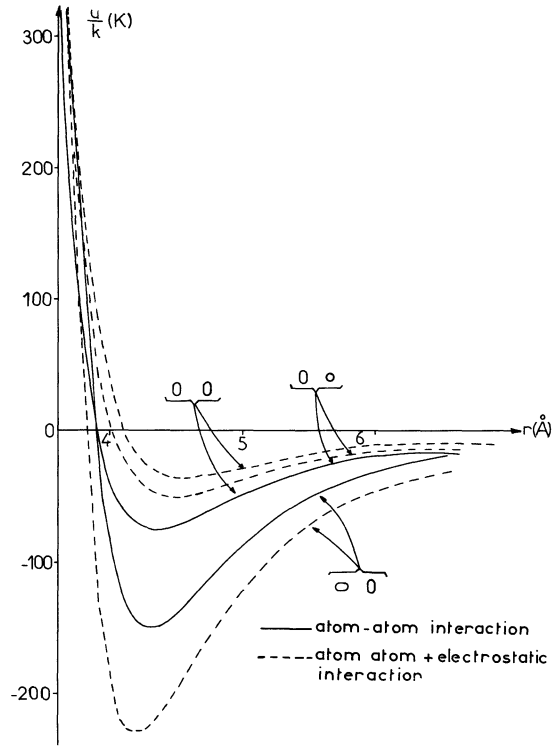

Fig. 8*b*. — The interaction energy between two CO molecules with three fixed orientations as a function of the intermolecular distance.

6. **Application to the line widths calculations.** — In this section we successively examine the self-broadening of the rotational Raman lines of N_2, CO_2 and CO and the broadening of the infrared vibration-rotation lines of pure CO and of CO-N_2 and CO-CO_2 gas mixtures. All the following numerical applications start from eq. (12) and its specification through eqs. (6) to (11) and Appendix C and A. The potential surfaces considered are the same as examined in section 5 for pure N_2, CO_2 and CO. For the gas mixtures the potential surfaces were derived in the same way using moreover the usual combination rules to determine the molecular parameters from the tabulated values of table II. In all the cases studied above the contribution of the vibrational effects in the fundamental band is noticeably small [64-66] (or zero for the rotational Raman lines since $v_i \equiv v_f$) and will be disregarded. This is equivalent to taking $S_{1,f2} = S_{1,i2}$ in eq. (12). In an analogous way we also use $S'_{2,f2} = S'_{2,i2}$ in this equation because of the very weak observed shifts [67] (even for the 0-2 harmonic band these shifts are hardly detectable). This experimental fact indicates at the same time that the vibrational effects are weak as just stated above and that the rotational contribution resulting from the non-commutation of the interaction at two different instants is also negligible [6]. We also mention that all the numerical line width calculations were performed by replacing the average over the relative velocities (cf. eq. (12)) by the average velocity approximation. The corresponding mean velocity was determined in each case for the temperature of the experiment considered.

Finally we point out that all the molecular constants used in these calculations (cf. table II) were obtained from sources independent of the pressure-broadening experiments (cf. sect. 5).

6.1 Rotational Raman lines of N_2, CO_2 and CO. — A detailed experimental study of the rotational Raman lines was realized by Jammu, St. John and Welsh [68] for pure N_2, CO_2 and CO. The impact theory of Fiutak and Van Kranendonk [3] was then applied [69, 70] to the broadening calculation of these observed lines by considering the quadrupolar and anisotropic dispersion interactions. Recall that this theory [3] is limited to second-order and requires, through a linear trajectory model with a constant velocity, a questionable cutoff procedure [7] for small impact parameters. Although the order of magnitude of these theoretical results was consistent with the experimental data, important discrepancies did appear mainly concerning the dependence of the broadening on the rotational quantum number j_i as evidenced on figures 9*a*, 9*b* and 9*c*. The results of our calculations were also reported on these figures (in the case of the rotational Raman lines $j_f = j_i + 2$ is found and the rank of the tensor characterizing the coupling between matter and radiation is two, i.e. $J = 2$ in eq. (11)). It is to be noted that our results are very consistent with experiments in the three cases.

6.2 Infrared vibration-rotation lines of pure CO and of CO-N_2 and CO-CO_2 mixtures. — The line widths of carbon monoxide pressure-broadened by itself and by many foreign gases (rare gases, N_2, CO_2, O_2, HCl, NO, etc...) were measured in various vibrational bands for several temperatures [65, 66, 67, 71, 72]. The measurements at low temperatures [71] (200 K < T < 250 K) are of planetary interest concerning the atmospheres of Mars and Venus. The previous attempts [65, 73] to calculate these line widths employed the Anderson theory and led Varanasi [8] to conclude that *a thorough revision of this*

Fig. 9. — The half-width at half-intensity γ of rotational Raman lines as a function of the rotational quantum number j_i (O : experimental values from ref. [68] ; ● : theoretical values from ref. [70] ; ▲ : calculated values from the present study ; △ : calculated values but without the $S_2^{(C)}$ and $S_2^{(L)}$ rotational dephasing contributions (cf. eq. (12)) disregarded in ref. [38]). 9*a*. — For N_2 gas ; 9*b*. — For CO_2 gas ; 9*c*. — For CO gas.

Fig. 10. — The half-width at half-intensity γ of fundamental vibration-rotation lines as a function of the rotational quantum number j_i for various temperatures (O : experimental values ; ▲ : calculated values from the present study). 10*a*. — For pure CO gas ; experimental values from ref. [71] ; 10*b*. — For CO-N_2 gas mixture ; experimental values from refs. [65] and [72] ; 10*c*. — For CO-CO_2 gas mixture ; experimental values from ref. [71].

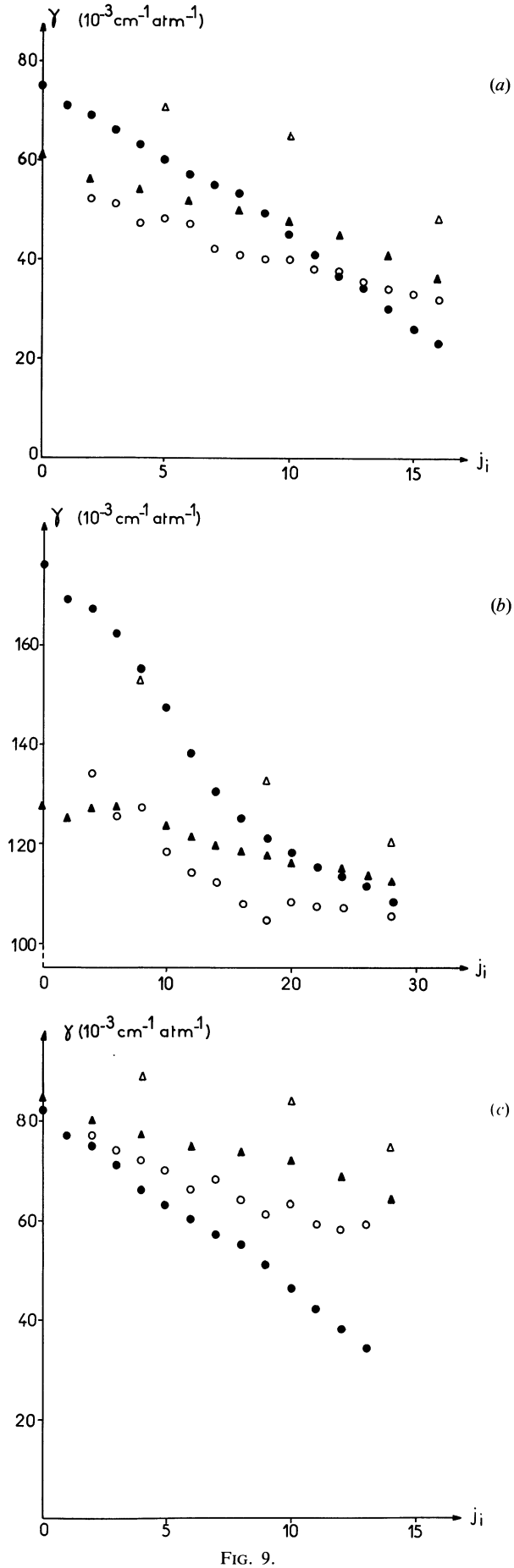
γ (10⁻³cm⁻¹atm⁻¹)
(a)
(b)
(c)
j_i

FIG. 9.

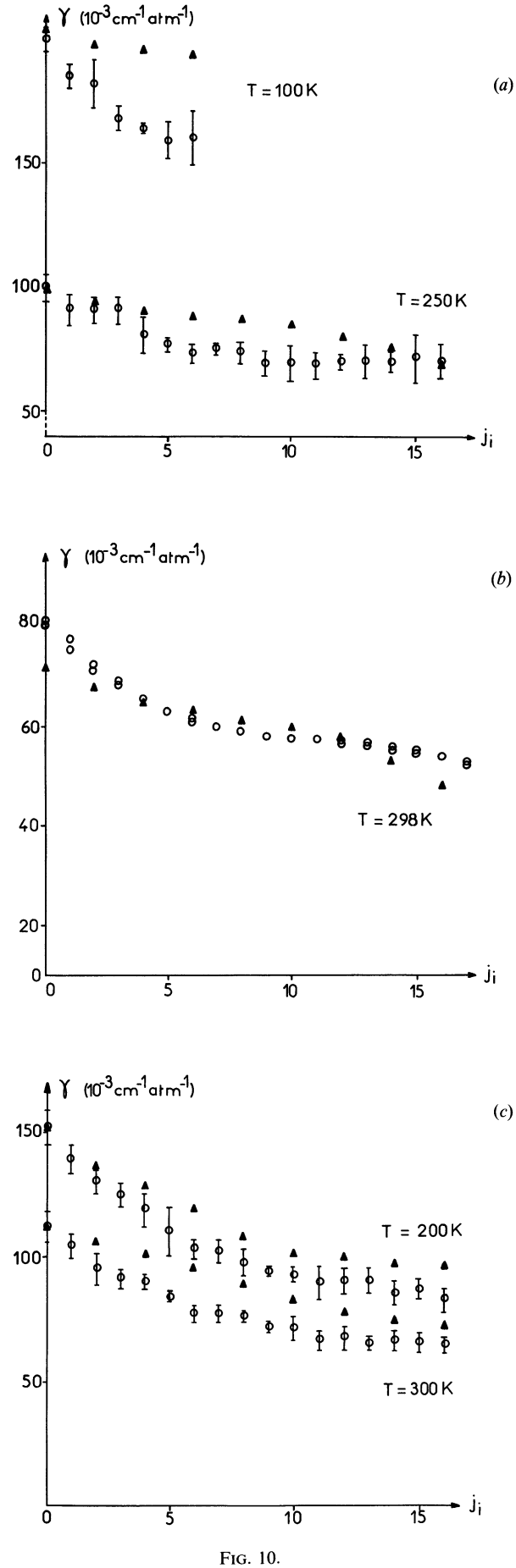
γ (10⁻³cm⁻¹atm⁻¹)
T = 100K
T = 250K
T = 298K
T = 200K
T = 300K
(a)
(b)
(c)
j_i

FIG. 10.

theory is required for all but simple dipole-dipole interactions. The present approach constitutes an attempt to answer this question and thus it is interesting to calculate the CO line widths within the theoretical frame developed above for various physical conditions. We have retained here only the three cases (CO-CO, CO-N_2 and CO-CO_2) for which the potential surfaces were determined with a sufficient credibility (cf. sect. 5). All the calculations were performed following the approach of the previous section (6.1) but with $j_f = j_i + 1$ (R branch) and $J = 1$ in eq. (11) (tensor rank of the dipolar coupling between matter and radiation). The available data for low temperatures [71] permit in that case an interesting application of our model, the previous calculations [8, 71] leading to increasing discrepancies for decreasing temperatures specially for high rotational quantum numbers j_i. Figures 9*a* to 9*c* show a comparison between the experimental data and our calculated values. A good agreement is obtained for each considered case and both the j-dependence and the variation of γ with temperature are well reproduced.

7. **Discussion and conclusion.** — The consistency obtained in all the physical situations studied between calculated and experimental values (cf. Figs. 9 and 10) must be connected to several physically meaningful aspects contained in the present approach :

i) the use of an exponential form (cf. eqs. (5) and (12)) which to some extent takes into account contributions of orders higher than two (this model being exact at infinite order for the pure vibrational dephasing contribution (cf. sect. 3)) ;

ii) the introduction of a parabolic trajectory model which is particularly convenient for describing the close collisions (cf. sect. 4) ;

iii) in connection with the above point, the consideration of realistic anisotropic short range forces through the atom-atom model (cf. sect. 5).

Of course, the use of the Anderson theory may lead to calculated numerical values relatively consistent with the experimental values. But it is pointed out that such a calculation has no physical meaning as soon as the dominant collisions correspond to impact parameters of the same order of magnitude or *a fortiori* lower than the kinetic diameter. We recall that this last situation arises for all diatom-atom collisions and also for diatom-diatom collisions for high rotational levels, except when a large dipole-dipole interaction takes place. The present theoretical approach constitutes a realistic model of calculation for molecular line broadening and shifting since it avoids the drastic drawbacks concerning close collisions.

Acknowledgments. — The authors wish to thank Prof. L. Galatry for his interest in this work and for reading the manuscript. They also acknowledge Drs. L. Bonamy and C. Boulet for interesting discussions during this work. The numerical calculations were made easier thanks to the friendly cooperation of Dr. C. Boulet. Finally the authors are grateful to Dr. D. Levesque for communicating helpful information on the atom-atom potential.

Appendix A

Resonance functions appearing in the differential cross sections $^{n_1 n_2}S_2[r_c(b)]$ in the parabolic trajectory description.

$$^{1,0}f_7^7(k) = \frac{e^{-2k}}{225}\left\{\left[k^3 + 6k^2 + 15k + 15 + \frac{1}{2}\left(1 - \frac{v_c^2}{v_c'^2}\right)(-k^3 + 3k + 3)\right]^2 + \frac{v_c^2}{v_c'^2}(k^3 + 3k^2 + 3k)^2\right\}$$

$$^{1,0}f_{12}^{12}(k) = \frac{1}{14\,745\,600}\left\{\left[k^6 K_6(k) + \frac{1}{2}\left(1 - \frac{v_c^2}{v_c'^2}\right)(11k^5 K_5(k) - k^6 K_6(k))\right]^2 + \frac{v_c^2}{v_c'^2}k^{12} K_5(k)^2\right\}$$

$$^{1,0}f_7^{12}(k) = \frac{e^{-k}}{57\,600}\left\{\left[k^6 K_6(k) + \frac{1}{2}\left(1 - \frac{v_c^2}{v_c'^2}\right)(11k^5 K_5(k) - k^6 K_6(k))\right] \times \right.$$
$$\left. \times \left[k^3 + 6k^2 + 15k + 15 + \frac{1}{2}\left(1 - \frac{v_c^2}{v_c'^2}\right)(-k^3 + 3k + 3)\right] + \frac{v_c^2}{v_c'^2}k^6 K_5(k)(k^3 + 3k^2 + 3k)\right\}$$

$$^{2,0}f_6^6(k) = \frac{e^{-2k}}{63}\left\{12(k^2 + 3k + 3)^2 + \frac{v_c^2}{v_c'^2}\left[(k^3 + 3k^2 + 3k)^2 + \frac{1}{4}\left(1 - \frac{v_c^2}{v_c'^2}\right)^2(-k^3 + 3k^2 + 3k)^2\right.\right.$$
$$+ \left(1 - \frac{v_c^2}{v_c'^2}\right)(k^3 + 3k^2 + 3k)(-k^3 + 3k^2 + 3k) - 6(k^2 + 3k + 3)(-k^3 + 3k + 3)$$
$$\left.\left. + \frac{v_c^2}{v_c'^2}(-k^3 + 3k + 3)^2\right]\right\}$$

$$
\begin{aligned}
{}^{2,0}f_{12}^{12}(k) = \frac{e^{-2k}}{33\,041\,925}\Bigg\{ & 48(k^5+15k^4+105k^3+420k^2+945k+945)^2 \\
& + \frac{v_c^2}{v_c'^2}\Bigg[(k^6+15k^5+105k^4+420k^3+945k^2+945k)^2 \\
& + \frac{1}{4}\left(1-\frac{v_c^2}{v_c'^2}\right)^2(-k^6-3k^5+15k^4+120k^3+315k^2+315k)^2 \\
& + \left(1-\frac{v_c^2}{v_c'^2}\right)(k^6+15k^5+105k^4+420k^3+945k^2+945k) \\
& \times(-k^6-3k^5+15k^4+120k^3+315k^2+315k) \\
& - 12(k^5+15k^4+105k^3+420k^2+945k+945) \\
& \times(-k^6-9k^5-30k^4+315k^2+945k+945) \\
& + \frac{v_c^2}{v_c'^2}(-k^6-9k^5-30k^4+315k^2+945k+945)^2\Bigg]\Bigg\}
\end{aligned}
$$

$$
\begin{aligned}
{}^{2,0}f_{6}^{12}(k) = \frac{e^{-2k}}{45\,360}\Bigg\{ & 24(k^2+3k+3)(k^5+15k^4+105k^3+420k^2+945k+945) \\
& + \frac{v_c^2}{v_c'^2}\Bigg[(k^3+3k^2+3k)(k^6+15k^5+105k^4+420k^3+945k^2+945k) \\
& + \frac{1}{4}\left(1-\frac{v_c^2}{v_c'^2}\right)^2(-k^3+3k^2+3k)(-k^6-3k^5+15k^4+120k^3+315k^2+315k) \\
& + \frac{1}{2}\left(1-\frac{v_c^2}{v_c'^2}\right)[(-k^3+3k^2+3k)(k^6+15k^5+105k^4+420k^3+945k^2+945k) \\
& + (k^3+3k^2+3k)(-k^6-3k^5+15k^4+120k^3+315k^2+315k)] \\
& - 3(k^2+3k+3)(-k^6-9k^5-30k^4+315k^2+945k+945) \\
& - 6(-k^3+3k+3)(k^5+15k^4+105k^3+420k^2+945k+945) \\
& + \frac{v_c^2}{v_c'^2}(-k^3+3k+3)(-k^6-9k^5-30k^4+315k^2+945k+945)\Bigg]\Bigg\}.
\end{aligned}
$$

For the other resonance f-functions appearing in the differential collision cross sections expressions (cf. App. C) (i.e. ${}^{1,1}f_3^3$, ${}^{1,2}f_4^4$, ${}^{2,1}f_4^4$, ${}^{2,2}f_5^5$, ${}^{1,0}f_7^{13}$, ${}^{1,0}f_{13}^{13}$, ${}^{1,0}f_9^9$, ${}^{1,0}f_9^{15}$, ${}^{1,0}f_{15}^{15}$, ${}^{2,0}f_8^8$, ${}^{2,0}f_8^{14}$, ${}^{2,0}f_{14}^{14}$, ${}^{1,1}f_8^8$, ${}^{1,1}f_8^{14}$, ${}^{1,1}f_{14}^{14}$, ${}^{1,2}f_9^9$, ${}^{1,2}f_9^{15}$, ${}^{1,2}f_{15}^{15}$, ${}^{2,1}f_9^9$, ${}^{2,1}f_9^{15}$, ${}^{2,1}f_{15}^{15}$, ${}^{2,2}f_{10}^{10}$, ${}^{2,2}f_{10}^{16}$, ${}^{2,2}f_{16}^{16}$, ${}^{1,0}f_7^9$, ${}^{1,0}f_{13}^{15}$, ${}^{1,0}f_7^{15}$, ${}^{1,0}f_9^{13}$, ${}^{1,1}f_3^8$, ${}^{1,1}f_3^{14}$, ${}^{1,2}f_4^9$, ${}^{1,2}f_4^{15}$, ${}^{2,1}f_4^9$, ${}^{2,1}f_4^{15}$, ${}^{2,2}f_5^{10}$, ${}^{2,2}f_5^{16}$) see J. Bonamy and D. Robert, Internal Report (1979), Laboratoire de Physique Moléculaire, Faculté des Sciences, 25030 Besançon Cedex, France.

Appendix B

Expressions of the ${}^{q}_{ij}D^{m_1m_2}_{l_1l_2}$ and ${}^{q}_{ij}E^{m_1m_2}_{l_1l_2}$ coefficients in terms of the molecular parameters r_{1i} and r_{2j} and of the $u_{l_1l_2m}(r)$ functions.

B$_1$ EVEN l_1 AND l_2

$$
{}^{0}_{ij}D^{00}_{00} = 4\pi \qquad {}^{0}_{ij}E^{00}_{00} = 4\pi
$$

$$
{}^{2}_{ij}D^{00}_{00} = 88\,\pi(r_{1i}^2+r_{2j}^2) \qquad {}^{2}_{ij}E^{00}_{00} = 20\,\pi(r_{1i}^2+r_{2j}^2)
$$

$$
{}^{2}_{ij}D^{00}_{20} = \frac{224\,\pi}{\sqrt{5}}r_{1i}^2 \qquad {}^{2}_{ij}E^{00}_{20} = \frac{64\,\pi}{\sqrt{5}}r_{1i}^2
$$

$$
{}^{4}_{ij}D^{00}_{00} = \frac{4\,004\,\pi}{5}\left(r_{1i}^4+r_{2j}^4+\frac{10}{3}r_{1i}^2r_{2j}^2\right) \qquad {}^{4}_{ij}E^{00}_{00} = 56\,\pi\left(r_{1i}^4+r_{2j}^4+\frac{10}{3}r_{1i}^2r_{2j}^2\right)
$$

$$
{}^{4}_{ij}D^{00}_{20} = \frac{2\,816\,\pi}{\sqrt{5}}\left(r_{1i}^4+\frac{7}{3}r_{1i}^2r_{2j}^2\right) \qquad {}^{4}_{ij}E^{00}_{20} = \frac{1\,600\,\pi}{7\sqrt{5}}\left(r_{1i}^4+\frac{7}{3}r_{1i}^2r_{2j}^2\right)
$$

$$ {}^{4}_{ij}D^{00}_{22} = \frac{50\,848\,\pi}{15} r^2_{1i} r^2_{2j} \qquad {}^{4}_{ij}E^{00}_{22} = \frac{5\,312\,\pi}{15} r^2_{1i} r^2_{2j} $$

$$ {}^{4}_{ij}D^{1-1}_{22} = {}^{4}_{ij}D^{-11}_{22} = \frac{3\,360\,\pi}{5} r^2_{1i} r^2_{2j} \qquad {}^{4}_{ij}E^{1-1}_{22} = {}^{4}_{ij}E^{-11}_{22} = \frac{576\,\pi}{5} r^2_{1i} r^2_{2j} $$

$$ {}^{4}_{ij}D^{2-2}_{22} = {}^{4}_{ij}D^{-22}_{22} = \frac{224\,\pi}{5} r^2_{1i} r^2_{2j} \qquad {}^{4}_{ij}E^{2-2}_{22} = {}^{4}_{ij}E^{-22}_{22} = \frac{64\,\pi}{5} r^2_{1i} r^2_{2j} $$

$$ {}^{4}_{ij}D^{00}_{40} = \frac{3\,072\,\pi}{5} r^4_{1i} \qquad {}^{4}_{ij}E^{00}_{40} = \frac{512\,\pi}{7} r^4_{1i} $$

$$ F^{00}_{22} = \frac{24\,\pi}{5} \qquad F^{1-1}_{22} = F^{-11}_{22} = \frac{16\,\pi}{5}. $$

$$ F^{2-2}_{22} = F^{-22}_{22} = \frac{4\,\pi}{5} $$

The approximate expressions for $u_{000}(r)$, $u_{200}(r)$, $u_{220}(r)$, $u_{221}(r)$ and $u_{222}(r)$ are given by (cf. eq. (33))

$$ u_{000}(r) = \sum_{ij} \left\{ \left[\frac{d_{ij}}{r^{12}} - \frac{e_{ij}}{r^6} \right] + (r^2_{1i} + r^2_{2j}) \left[\frac{22\,d_{ij}}{r^{14}} - \frac{5\,e_{ij}}{r^8} \right] + \left(r^4_{1i} + r^4_{2j} + \frac{10}{3} r^2_{1i} r^2_{2j} \right) \left[\frac{1\,001\,d_{ij}}{5\,r^{16}} - \frac{14\,e_{ij}}{r^{10}} \right] \right\} $$

$$ u_{200}(r) = \frac{1}{\sqrt{5}} \sum_{ij} \left\{ r^2_{1i} \left[\frac{56\,d_{ij}}{r^{14}} - \frac{16\,e_{ij}}{r^8} \right] + \left(r^4_{1i} + \frac{7}{3} r^2_{1i} r^2_{2j} \right) \left[\frac{704\,d_{ij}}{r^{16}} - \frac{400\,e_{ij}}{7\,r^{10}} \right] \right\} $$

$$ u_{220}(r) = \frac{1}{15} \sum_{ij} \left\{ r^2_{1i} r^2_{2j} \left[\frac{12\,712\,d_{ij}}{r^{16}} - \frac{1\,328\,e_{ij}}{r^{10}} \right] \right\} + \frac{6\,Q_1\,Q_2}{5\,r^5} $$

$$ u_{221}(r) = \frac{1}{5} \sum_{ij} \left\{ r^2_{1i} r^2_{2j} \left[\frac{840\,d_{ij}}{r^{16}} - \frac{144\,e_{ij}}{r^{10}} \right] \right\} + \frac{4\,Q_1\,Q_2}{5\,r^5} $$

$$ u_{222}(r) = \frac{1}{5} \sum_{ij} \left\{ r^2_{1i} r^2_{2j} \left[\frac{56\,d_{ij}}{r^{16}} - \frac{16\,e_{ij}}{r^{10}} \right] \right\} + \frac{Q_1\,Q_2}{5\,r^5} $$

$$ u_{400}(r) = \sum_{ij} \left\{ r^4_{1i} \left[\frac{768\,d_{ij}}{5\,r^{16}} - \frac{128\,e_{ij}}{7\,r^{10}} \right] \right\}. $$

B_2 Odd l_1 or l_2

$$ {}^{1}_{ij}D^{00}_{10} = \frac{48\,\pi}{\sqrt{3}} r_{1i} \qquad {}^{1}_{ij}E^{00}_{10} = \frac{24\,\pi}{\sqrt{3}} r_{1i} $$

$$ {}^{2}_{ij}D^{00}_{11} = -\,208\,\pi r_{1i} r_{2j} \qquad {}^{2}_{ij}E^{00}_{11} = -\,56\,\pi r_{1i} r_{2j} $$

$$ {}^{2}_{ij}D^{1-1}_{11} = {}^{2}_{ij}D^{-11}_{11} = -\,16\,\pi r_{1i} r_{2j} \qquad {}^{2}_{ij}E^{1-1}_{11} = {}^{2}_{ij}E^{-11}_{11} = -\,8\,\pi r_{1i} r_{2j} $$

$$ {}^{3}_{ij}D^{00}_{10} = \frac{1\,232\,\pi}{\sqrt{3}} \left(\frac{3}{5} r^3_{1i} + r_{1i} r^2_{2j} \right) \qquad {}^{3}_{ij}E^{00}_{10} = \frac{160\,\pi}{\sqrt{3}} \left(\frac{3}{5} r^3_{1i} + r_{1i} r^2_{2j} \right) $$

$$ {}^{3}_{ij}D^{00}_{12} = \frac{3\,136\,\pi}{\sqrt{15}} r_{1i} r^2_{2j} \qquad {}^{3}_{ij}E^{00}_{12} = \frac{512\,\pi}{\sqrt{15}} r_{1i} r^2_{2j} $$

$$ {}^{3}_{ij}D^{00}_{21} = -\,\frac{3\,136\,\pi}{\sqrt{15}} r^2_{1i} r_{2j} \qquad {}^{3}_{ij}E^{00}_{21} = -\,\frac{512\,\pi}{\sqrt{15}} r^2_{1i} r_{2j} $$

$$ {}^{3}_{ij}D^{1-1}_{12} = {}^{3}_{ij}D^{-11}_{12} = \frac{224\,\pi}{\sqrt{5}} r_{1i} r^2_{2j} \qquad {}^{3}_{ij}E^{1-1}_{12} = {}^{3}_{ij}E^{-11}_{12} = \frac{64\,\pi}{\sqrt{5}} r_{1i} r^2_{2j} $$

$$ {}^{3}_{ij}D^{1-1}_{21} = {}^{3}_{ij}D^{-11}_{21} = -\,\frac{224\,\pi}{\sqrt{5}} r^2_{1i} r_{2j} \qquad {}^{3}_{ij}E^{1-1}_{21} = {}^{3}_{ij}E^{-11}_{21} = -\,\frac{64\,\pi}{\sqrt{5}} r^2_{1i} r_{2j} $$

$$G_{11}^{00} = -\frac{8\pi}{3} \qquad G_{11}^{1-1} = G_{11}^{-11} = -\frac{4\pi}{3}$$

$$H_{12}^{00} = 4\pi\sqrt{\frac{3}{5}} \qquad H_{12}^{1-1} = H_{12}^{-11} = \frac{4\pi}{\sqrt{5}}$$

$$I_{21}^{00} = -4\pi\sqrt{\frac{3}{5}} \qquad I_{21}^{1-1} = I_{21}^{-11} = -\frac{4\pi}{\sqrt{5}}$$

(*N.B.* The G, H and I coefficients are defined in analogy with F coefficients of eq. (33) but refer to $\frac{\mu_1\mu_2}{r^3}$, $\frac{\mu_1 Q_2}{r^4}$ and $\frac{\mu_2 Q_1}{r^4}$ respectively instead of $\frac{Q_1 Q_2}{r^5}$).

The corresponding $u_{l_1 l_2 m}(r)$ functions are defined through

$$u_{100}(r) = \frac{1}{\sqrt{3}}\sum_{ij}\left\{r_{1i}\left[\frac{12\,d_{ij}}{r^{13}} - \frac{6\,e_{ij}}{r^7}\right] + \left(\frac{3}{5}r_{1i}^3 + r_{1i}r_{2j}^2\right)\left[\frac{308\,d_{ij}}{r^{15}} - \frac{40\,e_{ij}}{r^9}\right]\right\}$$

$$u_{110}(r) = \sum_{ij}\left\{-r_{1i}r_{2j}\left[\frac{52\,d_{ij}}{r^{14}} - \frac{14\,e_{ij}}{r^8}\right]\right\} - \frac{2}{3}\frac{\mu_1\mu_2}{r^3}$$

$$u_{111}(r) = \sum_{ij}\left\{-r_{1i}r_{2j}\left[\frac{4\,d_{ij}}{r^{14}} - \frac{2\,e_{ij}}{r^8}\right]\right\} - \frac{\mu_1\mu_2}{3r^3}$$

$$u_{210}(r) = \frac{1}{\sqrt{15}}\sum_{ij}\left\{-r_{1i}^2 r_{2j}\left[\frac{784\,d_{ij}}{r^{15}} - \frac{128\,e_{ij}}{r^9}\right]\right\} - \sqrt{\frac{3}{5}}\frac{\mu_2 Q_1}{r^4}$$

$$u_{120}(r) = \frac{1}{\sqrt{15}}\sum_{ij}\left\{r_{1i}r_{2j}^2\left[\frac{784\,d_{ij}}{r^{15}} - \frac{128\,e_{ij}}{r^9}\right]\right\} + \sqrt{\frac{3}{5}}\frac{\mu_1 Q_2}{r^4}$$

$$u_{211}(r) = \frac{1}{\sqrt{5}}\sum_{ij}\left\{-r_{1i}^2 r_{2j}\left[\frac{56\,d_{ij}}{r^{15}} - \frac{16\,e_{ij}}{r^9}\right]\right\} - \frac{1}{\sqrt{5}}\frac{\mu_2 Q_1}{r^4}$$

$$u_{121}(r) = \frac{1}{\sqrt{5}}\sum_{ij}\left\{r_{1i}r_{2j}^2\left[\frac{56\,d_{ij}}{r^{15}} - \frac{16\,e_{ij}}{r^9}\right]\right\} + \frac{1}{\sqrt{5}}\frac{\mu_1 Q_2}{r^4}$$

(*N.B.* : We recall that r_{1i} and r_{2j} are *algebraic* quantities, cf. figure 5.)

Appendix C

Expressions of the $S_2[r_c(b)]$ and $S_2^{(L)}[r_c(b)]$ functions (we recall (cf. eq. (7)) that

$$S_2[r_c(b)] = S_{2,f2} + S_{2,i2} + S_{2,f2i2}^{(C)}$$

where each term is defined by eqs. (9) and (11)).

ELECTROSTATIC CONTRIBUTIONS

$$^{1,1}S_2[r_c(b)] = \frac{4}{9}\left(\frac{\mu_1\mu_2}{\hbar v_c'}\right)^2\frac{1}{r_c^4}\left\{\sum_{j_1',j_2'} C_{j_1'}^{(1)}C_{j_2'}^{(1)\,1,1}f_3^3(k) + \sum_{j_f',j_2'} C_{j_f'}^{(1)}C_{j_2'}^{(2)\,1,1}f_3^3(k)\right\}$$

$$^{1,2}S_2[r_c(b)] = \frac{16}{45}\left(\frac{\mu_1 Q_2}{\hbar v_c'}\right)^2\frac{1}{r_c^6}\left\{\sum_{j_1',j_2'} C_{j_1'}^{(1)}C_{j_2'}^{(2)\,1,2}f_4^4(k) + \sum_{j_f',j_2'} C_{j_f'}^{(1)}C_{j_2'}^{(2)\,1,2}f_4^4(k)\right\}$$

$$^{2,1}S_2[r_c(b)] = \frac{16}{45}\left(\frac{\mu_2 Q_1}{\hbar v_c'}\right)^2\frac{1}{r_c^6}\left\{\sum_{j_1',j_2'} C_{j_1'}^{(2)}C_{j_2'}^{(1)\,2,1}f_4^4(k) + \sum_{j_f',j_2'} C_{j_f'}^{(2)}C_{j_2'}^{(1)\,2,1}f_4^4(k)\right\}$$

$$^{2,1}S_2^{(L)}[r_c(b)] = \frac{16}{45}\left(\frac{\mu_2 Q_1}{\hbar v_c'}\right)^2 \frac{1}{r_c^6} D \sum_{j_2' \neq j_2} C_{j_2}^{(1)\ 2,1} f_4^4(k)$$

$$^{2,2}S_2[r_c(b)] = \frac{16}{25}\left(\frac{Q_1 Q_2}{\hbar v_c'}\right)^2 \frac{1}{r_c^8}\left\{\sum_{j_1',j_2'} C_{j_1'}^{(2)} C_{j_2'}^{(2)\ 2,2} f_5^5(k) + \sum_{j_1',j_2'} C_{j_1'}^{(2)} C_{j_2'}^{(2)\ 2,2} f_5^5(k) + D C_{j_2'}^{(2)\ 2,2} f_5^5(k)\right\}$$

$$^{2,2}S_2^{(L)}[r_c(b)] = \frac{16}{25}\left(\frac{Q_1 Q_2}{\hbar v_c'}\right)^2 \frac{1}{r_c^8} D \sum_{j_2' \neq j_2} C_{j_2'}^{(2)\ 2,2} f_5^5(k) .$$

ATOM- ATOM CONTRIBUTIONS

$$^{1,0}S_2[r_c(b)] = \frac{75}{128}\left(\frac{\pi}{\hbar v_c'}\right)^2 \left\{\left(\sum_{ij} r_{1i}\, e_{ij}\right)^2 \frac{1}{r_c^{12}}\left(\sum_{j_1'} C_{j_1'}^{(1)\ 1,0} f_7^7(k) + \sum_{j_1'} C_{j_1'}^{(1)\ 1,0} f_7^7(k)\right)\right.$$
$$- \frac{231}{80}\left(\sum_{ij} r_{1i}\, e_{ij}\right)\left(\sum_{ij} r_{1i}\, d_{ij}\right)\frac{1}{r_c^{18}}\left(\sum_{j_1'} C_{j_1'}^{(1)\ 1,0} f_7^{13}(k) + \sum_{j_1'} C_{j_1'}^{(1)\ 1,0} f_7^{13}(k)\right)$$
$$\left. + \frac{53\,361}{25\,600}\left(\sum_{ij} r_{1i}\, d_{ij}\right)^2 \frac{1}{r_c^{24}}\left(\sum_{j_1'} C_{j_1'}^{(1)\ 1,0} f_{13}^{13}(k) + \sum_{j_1'} C_{j_1'}^{(1)\ 1,0} f_{13}^{13}(k)\right)\right\}$$

$$^{1,0}S_2[r_c(b)] = \frac{30\,625}{1\,536}\left(\frac{\pi}{\hbar v_c}\right)^2 \left\{\left(\sum_{ij}\left(\frac{3}{5} r_{1i}^3\, e_{ij} + r_{1i}\, r_{2j}^2\, e_{ij}\right)\right)^2 \frac{1}{r_c^{16}}\left(\sum_{j_1'} C_{j_1'}^{(1)\ 1,0} f_9^9(k) + \sum_{j_1'} C_{j_1'}^{(1)\ 1,0} f_9^9(k)\right)\right.$$
$$- \frac{4\,719}{400}\left(\sum_{ij}\left(\frac{3}{5} r_{1i}^3\, e_{ij} + r_{1i}\, r_{2j}^2\, e_{ij}\right)\right)\left(\sum_{ij}\left(\frac{3}{5} r_{1i}^3\, d_{ij} + r_{1i}\, r_{2j}^2\, d_{ij}\right)\right)$$
$$\times \frac{1}{r_c^{22}}\left(\sum_{j_1'} C_{j_1'}^{(1)\ 1,0} f_9^{15}(k) + \sum_{j_1'} C_{j_1'}^{(1)\ 1,0} f_9^{15}(k)\right) + \frac{22\,268\,961}{640\,000}\left(\sum_{ij}\left(\frac{3}{5} r_{1i}^3\, d_{ij} + r_{1i}\, r_{2j}^2\, d_{ij}\right)\right)^2$$
$$\left. \times \frac{1}{r_c^{28}}\left(\sum_{j_1'} C_{j_1'}^{(1)\ 1,0} f_{15}^{15}(k) + \sum_{j_1'} C_{j_1'}^{(1)\ 1,0} f_{15}^{15}(k)\right)\right\}$$

$$^{2,0}S_2[r_c(b)] = \frac{9\,675}{5\,760}\left(\frac{\pi}{\hbar v_c'}\right)^2 \left\{\left(\sum_{ij} r_{1i}^2\, e_{ij}\right)^2 \frac{1}{r_c^{14}}\left(\sum_{j_1'} C_{j_1'}^{(2)\ 2,0} f_8^8(k) + \sum_{j_1'} C_{j_1'}^{(2)\ 2,0} f_8^8(k) + D\right)\right.$$
$$- \frac{9\,471}{1\,720}\left(\sum_{ij} r_{1i}^2\, e_{ij}\right)\left(\sum_{ij} r_{1i}^2\, d_{ij}\right)\frac{1}{r_c^{20}}\left(\sum_{j_1'} C_{j_1'}^{(2)\ 2,0} f_8^{14}(k) + \sum_{j_1'} C_{j_1'}^{(2)\ 2,0} f_8^{14}(k) + D\right)$$
$$\left. + \frac{8\,377\,677}{1\,100\,800}\left(\sum_{ij} r_{1i}^2\, d_{ij}\right)^2 \frac{1}{r_c^{26}}\left(\sum_{j_1'} C_{j_1'}^{(2)\ 2,0} f_{14}^{14}(k) + \sum_{j_1'} C_{j_1'}^{(2)\ 2,0} f_{14}^{14}(k) + D\right)\right\}$$

$$^{1,1}S_2[r_c(b)] = \frac{925}{128}\left(\frac{\pi}{\hbar v_c'}\right)^2 \left\{\left(\sum_{ij} r_{1i}\, r_{2j}\, e_{ij}\right)^2 \frac{1}{r_c^{14}}\left(\sum_{j_1',j_2'} C_{j_1'}^{(1)} C_{j_2'}^{(1)\ 1,1} f_8^8(k) + \sum_{j_1',j_2'} C_{j_1'}^{(1)} C_{j_2'}^{(1)\ 1,1} f_8^8(k)\right)\right.$$
$$- \frac{16\,863}{2\,960}\left(\sum_{ij} r_{1i}\, r_{2j}\, e_{ij}\right)\left(\sum_{ij} r_{1i}\, r_{2j}\, d_{ij}\right)$$
$$\times \frac{1}{r_c^{20}}\left(\sum_{j_1',j_2'} C_{j_1'}^{(1)} C_{j_2'}^{(1)\ 1,1} f_8^{14}(k) + \sum_{j_1',j_2'} C_{j_1'}^{(1)} C_{j_2'}^{(1)\ 1,1} f_8^{14}(k)\right) + \frac{1\,547\,469}{189\,440}\left(\sum_{ij} r_{1i}\, r_{2j}\, d_{ij}\right)^2$$
$$\left. \times \frac{1}{r_c^{26}}\left(\sum_{j_1',j_2'} C_{j_1'}^{(1)} C_{j_2'}^{(1)\ 1,1} f_{14}^{14}(k) + \sum_{j_1',j_2'} C_{j_1'}^{(1)} C_{j_2'}^{(1)\ 1,1} f_{14}^{14}(k)\right)\right\}$$

$$^{1,2}S_2[r_c(b)] = \frac{5\,635}{192}\left(\frac{\pi}{\hbar v_c'}\right)^2 \left\{\left(\sum_{ij} r_{1i}\, r_{2j}^2\, e_{ij}\right)^2 \frac{1}{r_c^{16}}\left(\sum_{j_1',j_2'} C_{j_1'}^{(1)} C_{j_2'}^{(2)\ 1,2} f_9^9(k) + \sum_{j_1',j_2'} C_{j_1'}^{(1)} C_{j_2'}^{(2)\ 1,2} f_9^9(k)\right)\right.$$
$$- \frac{7\,293}{1\,472}\left(\sum_{ij} r_{1i}\, r_{2j}^2\, e_{ij}\right)\left(\sum_{ij} r_{1i}\, r_{2j}^2\, d_{ij}\right)\frac{1}{r_c^{22}}\left(\sum_{j_1',j_2'} C_{j_1'}^{(1)} C_{j_2'}^{(2)\ 1,2} f_9^{15}(k) + \sum_{j_1',j_2'} C_{j_1'}^{(1)} C_{j_2'}^{(2)\ 1,2} f_9^{15}(k)\right)$$
$$\left. + \frac{184\,041}{7\,360}\left(\sum_{ij} r_{1i}\, r_{2j}^2\, d_{ij}\right)^2 \frac{1}{r_c^{28}}\left(\sum_{j_1',j_2'} C_{j_1'}^{(1)} C_{j_2'}^{(2)\ 1,2} f_{15}^{15}(k) + \sum_{j_1',j_2'} C_{j_1'}^{(1)} C_{j_2'}^{(2)\ 1,2} f_{15}^{15}(k)\right)\right\}$$

$$
{}^{2,1}S_2[r_c(b)] = \frac{5\,635}{192}\left(\frac{\pi}{\hbar v_c'}\right)^2 \left\{\left(\sum_{ij} r_{1i}^2\, r_{2j}\, e_{ij}\right)^2 \frac{1}{r_c^{16}}\left(\sum_{j_1',j_2'} C_{j_1'}^{(2)}\, C_{j_2'}^{(1)}\, {}^{2,1}f_9^9(k) + \sum_{j_1',j_2'} C_{j_1'}^{(2)}\, C_{j_2'}^{(1)}\, {}^{2,1}f_9^9(k)\right)\right.
$$
$$
- \frac{7\,293}{736}\left(\sum_{ij} r_{1i}^2\, r_{2j}\, e_{ij}\right)\left(\sum_{ij} r_{1i}^2\, r_{2j}\, d_{ij}\right)\frac{1}{r_c^{22}}\left(\sum_{j_1',j_2'} C_{j_1'}^{(2)}\, C_{j_2'}^{(1)}\, {}^{2,1}f_9^{15}(k) + \sum_{j_1',j_2'} C_{j_1'}^{(2)}\, C_{j_2'}^{(1)}\, {}^{2,1}f_9^{15}(k)\right)
$$
$$
\left. + \frac{184\,041}{7\,360}\left(\sum_{ij} r_{1i}^2\, r_{2j}\, d_{ij}\right)^2 \frac{1}{r_c^{28}}\left(\sum_{j_1',j_2'} C_{j_1'}^{(2)}\, C_{j_2'}^{(1)}\, {}^{2,1}f_{15}^{15}(k) + \sum_{j_1',j_2'} C_{j_1'}^{(2)}\, C_{j_2'}^{(1)}\, {}^{2,1}f_{15}^{15}(k)\right)\right\}
$$

$$
{}^{2,1}S_2^{(L)}[r_c(b)] = \frac{5\,635}{192}\left(\frac{\pi}{\hbar v_c'}\right)^2 D \sum_{j_2' \neq j_2} C_{j_2'}^{(1)} \left\{\left(\sum_{ij} r_{1i}^2\, r_{2j}\, e_{ij}\right)^2 \frac{1}{r_c^{16}}\, {}^{2,1}f_9^9(k) - \frac{7\,293}{736}\left(\sum_{ij} r_{1i}^2\, r_{2j}\, e_{ij}\right) \times\right.
$$
$$
\left. \times \left(\sum_{ij} r_{1i}^2\, r_{2j}\, d_{ij}\right)\frac{1}{r_c^{22}}\, {}^{2,1}f_9^{15}(k) + \frac{184\,041}{7\,360}\left(\sum_{ij} r_{1i}^2\, r_{2j}\, d_{ij}\right)^2 \frac{1}{r_c^{28}}\, {}^{2,1}f_{15}^{15}(k)\right\}
$$

$$
{}^{2,2}S_2[r_c(b)] = \frac{192\,913}{1\,152}\left(\frac{\pi}{\hbar v_c'}\right)^2 \left\{\left(\sum_{ij} r_{1i}^2\, r_{2j}^2\, e_{ij}\right)^2 \frac{1}{r_c^{18}}\left(\sum_{j_1',j_2'} C_{j_1'}^{(2)}\, C_{j_2'}^{(2)}\, {}^{2,2}f_{10}^{10}(k) + \right.\right.
$$
$$
\left. + \sum_{j_1',j_2'} C_{j_1'}^{(2)}\, C_{j_2'}^{(2)}\, {}^{2,2}f_{10}^{10}(k) + DC_{j_2'}^{(2)}\, {}^{2,2}f_{10}^{10}(k)\right) - \frac{6\,969\,963}{440\,944}\left(\sum_{ij} r_{1i}^2\, r_{2j}^2\, e_{ij}\right)
$$
$$
\times \left(\sum_{ij} r_{1i}^2\, r_{2j}^2\, d_{ij}\right)\frac{1}{r_c^{24}}\left(\sum_{j_1',j_2'} C_{j_1'}^{(2)}\, C_{j_2'}^{(2)}\, {}^{2,2}f_{10}^{16}(k) + \sum_{j_1',j_2'} C_{j_1'}^{(2)}\, C_{j_2'}^{(2)}\, {}^{2,2}f_{10}^{16}(k) + DC_{j_2'}^{(2)}\, {}^{2,2}f_{10}^{16}(k)\right)
$$
$$
+ \frac{6\,538\,424\,607}{100\,787\,200}\left(\sum_{ij} r_{1i}^2\, r_{2j}^2\, d_{ij}\right)^2 \frac{1}{r_c^{30}}\left(\sum_{j_1'j_2'} C_{j_1'}^{(2)}\, C_{j_2'}^{(2)}\, {}^{2,2}f_{16}^{16}(k)\right.
$$
$$
\left.\left. + \sum_{j_1',j_2'} C_{j_1'}^{(2)}\, C_{j_2'}^{(2)}\, {}^{2,2}f_{16}^{16}(k) + DC_{j_2'}^{(2)}\, {}^{2,2}f_{16}^{16}(k)\right)\right\}
$$

$$
{}^{2,2}S_2^{(L)}[r_c(b)] = \frac{192\,913}{1\,152}\left(\frac{\pi}{\hbar v_c'}\right)^2 D \sum_{j_2' \neq j_2} C_{j_2'}^{(2)} \left\{\left(\sum_{ij} r_{1i}^2\, r_{2j}^2\, e_{ij}\right)^2 \frac{1}{r_c^{18}}\, {}^{2,2}f_{10}^{10}(k) - \frac{6\,969\,963}{440\,944} \times\right.
$$
$$
\left. \times \left(\sum_{ij} r_{1i}^2\, r_{2j}^2\, e_{ij}\right)\left(\sum_{ij} r_{1i}^2\, r_{2j}^2\, d_{ij}\right)\frac{1}{r_c^{24}}\, {}^{2,2}f_{10}^{16}(k) + \frac{6\,538\,424\,607}{100\,787\,200}\left(\sum_{ij} r_{1i}^2\, r_{2j}^2\, d_{ij}\right)^2 \frac{1}{r_c^{30}}\, {}^{2,2}f_{16}^{16}(k)\right\}
$$

CROSS CONTRIBUTIONS

$$
{}^{1,0}S_2[r_c(b)] = \left(\frac{\pi}{\hbar v_c'}\right)^2 \left\{\frac{875}{128}\left(\sum_{ij} r_{1i}\, e_{ij}\right)\left(\sum_{ij}\left(\frac{3}{5} r_{1i}^3\, e_{ij} + r_{1i}\, r_{2j}^2\, e_{ij}\right)\right)\frac{1}{r_c^{14}}\left(\sum_{j_1'} C_{j_1'}^{(1)}\, {}^{1,0}f_7^9(k) + \sum_{=i'} C_{j_1'}^{(1)}\, {}^{1,0}f_7^9(k)\right)\right.
$$
$$
+ \frac{7\,630\,623}{131\,072}\left(\sum_{ij} r_{1i}\, d_{ij}\right)\left(\sum_{ij}\left(\frac{3}{5} r_{1i}^3\, d_{ij} + r_{1i}\, r_{2j}^2\, d_{ij}\right)\right)
$$
$$
\times \frac{1}{r_c^{26}}\left(\sum_{j_1'} C_{j_1'}^{(1)}\, {}^{1,0}f_{13}^{15}(k) + \sum_{j_1'} C_{j_1'}^{(1)}\, {}^{1,0}f_{13}^{15}(k)\right) - \frac{165\,165}{4\,096}\left(\sum_{ij} r_{1i}\, e_{ij}\right)\left(\sum_{ij}\left(\frac{3}{5} r_{1i}^3\, d_{ij} + r_{1i}\, r_{2j}^2\, d_{ij}\right)\right)
$$
$$
\times \frac{1}{r_c^{20}}\left(\sum_{j_1'} C_{j_1'}^{(1)}\, {}^{1,0}f_7^{15}(k) + \sum_{j_1'} C_{j_1'}^{(1)}\, {}^{1,0}f_7^{15}(k)\right) - \frac{40\,425}{4\,096}\left(\sum_{ij} r_{1i}\, d_{ij}\right)
$$
$$
\left.\times \left(\sum_{ij}\left(\frac{3}{5} r_{1i}^3\, e_{ij} + r_{1i}\, r_{2j}^2\, e_{ij}\right)\right)\frac{1}{r_c^{20}}\left(\sum_{j_1'} C_{j_1'}^{(1)}\, {}^{1,0}f_9^{13}(k) + \sum_{j_1'} C_{j_1'}^{(1)}\, {}^{1,0}f_9^{13}(k)\right)\right\}
$$

$$
{}^{1,1}S_2[r_c(b)] = \frac{\pi\mu_1\,\mu_2}{(\hbar v_c')^2}\left\{\frac{35}{12}\left(\sum_{ij} - r_{1i}\, r_{2j}\, e_{ij}\right)\frac{1}{r_c^9}\left(\sum_{j_1',j_2'} C_{j_1'}^{(1)}\, C_{j_2'}^{(1)}\, {}^{1,1}f_3^8(k) + \sum_{j_1',j_2'} C_{j_1'}^{(1)}\, C_{j_2'}^{(1)}\, {}^{1,1}f_3^8(k)\right)\right.
$$
$$
\left. - \frac{1\,001}{128}\left(\sum_{ij} - r_{1i}\, r_{2j}\, d_{ij}\right)\frac{1}{r^{15}}\left(\sum_{j_1',j_2'} C_{j_1'}^{(1)}\, C_{j_2'}^{(1)}\, {}^{1,1}f_3^{14}(k) + \sum_{j_1',j_2'} C_{j_1'}^{(1)}\, C_{j_2'}^{(1)}\, {}^{1,1}f_3^{14}(k)\right)\right\}
$$

$$
{}^{1,2}S_2[r_c(b)] = \frac{\pi\mu_1\, Q_2}{(\hbar v_c')^2}\left\{-\frac{21}{4}\left(\sum_{ij} r_{1i}\, r_{2j}^2\, e_{ij}\right)\frac{1}{r_c^{11}}\left(\sum_{j_1',j_2'} C_{j_1'}^{(1)}\, C_{j_2'}^{(2)}\, {}^{1,2}f_4^9(k) + \sum_{j_1',j_2'} C_{j_1'}^{(1)}\, C_{j_2'}^{(2)}\, {}^{1,2}f_4^9(k)\right)\right.
$$
$$
\left. + \frac{3\,003}{128}\left(\sum_{ij} r_{1i}\, r_{2j}^2\, d_{ij}\right)\frac{1}{r_c^{17}}\left(\sum_{j_1',j_2'} C_{j_1'}^{(1)}\, C_{j_2'}^{(2)}\, {}^{1,2}f_4^{15}(k) + \sum_{j_1',j_2'} C_{j_1'}^{(1)}\, C_{j_2'}^{(2)}\, {}^{1,2}f_4^{15}(k)\right)\right\}
$$

$$
{}^{2,1}S_2[r_c(b)] = \frac{\pi\mu_2 Q_1}{(\hbar v_c')^2}\left\{\frac{21}{4}\left(\sum_{ij} r_{1i}^2\, r_{2j}\, e_{ij}\right)\frac{1}{r_c^{11}}\left(\sum_{j_i,j_2'} C_{j_i}^{(2)}\, C_{j_2'}^{(1)}\, {}^{2,1}f_4^9(k) + \sum_{j_f,j_2'} C_{j_f}^{(2)}\, C_{j_2'}^{(1)}\, {}^{2,1}f_4^9(k)\right)\right.
$$
$$
\left. - \frac{3\,003}{128}\left(\sum_{ij} r_{1i}^2\, r_{2j}\, d_{ij}\right)\frac{1}{r_c^{17}}\left(\sum_{j_i,j_2'} C_{j_i}^{(2)}\, C_{j_2'}^{(1)}\, {}^{2,1}f_4^{15}(k) + \sum_{j_f,j_2'} C_{j_f}^{(2)}\, C_{j_2'}^{(1)}\, {}^{2,1}f_4^{15}(k)\right)\right\}
$$

$$
{}^{2,1}S_2^{(L)}[r_c(b)] = \frac{\pi\mu_2 Q_1}{(\hbar v_c')^2} D \sum_{j_2'\neq j_2} C_{j_2'}^{(1)}\left\{\frac{21}{4}\left(\sum_{ij} r_{1i}^2\, r_{2j}\, e_{ij}\right)\frac{1}{r_c^{11}}\,{}^{2,1}f_4^9(k) - \frac{3\,003}{128}\left(\sum_{ij} r_{1i}^2\, r_{2j}\, d_{ij}\right)\frac{1}{r_c^{17}}\,{}^{2,1}f_4^{15}(k)\right\}
$$

$$
{}^{2,2}S_2[r_c(b)] = \frac{\pi Q_1 Q_2}{(\hbar v_c')^2}\left\{-\frac{17\,073}{160}\left(\sum_{ij} r_{1i}^2\, r_{2j}^2\, e_{ij}\right)\frac{1}{r_c^{13}}\left(\sum_{j_i,j_2'} C_{j_i}^{(2)}\, C_{j_2'}^{(2)}\, {}^{2,2}f_5^{10}(k)\right.\right.
$$
$$
\left. + \sum_{j_f,j_2'} C_{j_f}^{(2)}\, C_{j_2'}^{(2)}\, {}^{2,2}f_5^{10}(k) + DC_{j_2'}^{(2)}\, {}^{2,2}f_5^{10}(k)\right) + \frac{153\,153}{1\,280}\left(\sum_{ij} r_{1i}^2\, r_{2j}^2\, d_{ij}\right)
$$
$$
\left.\times \frac{1}{r_c^{19}}\left(\sum_{j_i,j_2'} C_{j_i}^{(2)}\, C_{j_2'}^{(2)}\, {}^{2,2}f_5^{16}(k) + \sum_{j_f,j_2'} C_{j_f}^{(2)}\, C_{j_2'}^{(2)}\, {}^{2,2}f_5^{16}(k) + DC_{j_2'}^{(2)}\, {}^{2,2}f_5^{16}(k)\right)\right\}
$$

$$
{}^{2,2}S^{(L)}[r_c(b)] = \frac{\pi Q_1 Q_2}{(\hbar v_c')^2} D \sum_{j_2'\neq j_2} C_{j_2'}^{(2)}\left\{-\frac{17\,073}{160}\left(\sum_{ij} r_{1i}^2\, r_{2j}^2\, e_{ij}\right)\frac{1}{r_c^{13}}\,{}^{2,2}f_5^{10}(k)\right.
$$
$$
\left. + \frac{153\,153}{1\,280}\left(\sum_{ij} r_{1i}^2\, r_{2j}^2\, d_{ij}\right)\frac{1}{r_c^{19}}\,{}^{2,2}f_5^{16}(k)\right\}\ .
$$

In all the above equations we recall that $D = (-1)^{j_i+j_f}\, 2[(2j_i+1)(2j_f+1)\, C_{j_i}^{(2)}\, C_{j_f}^{(2)}]^{1/2} \times W(j_i j_f j_i j_f ; J2)$ where W is the Racah coefficient and J the order of the coupling tensor between the molecules and the external field.

References

[1] ANDERSON, P. W., *Phys. Rev.* **76** (1949) 647.
[2] TSAO, C. J. and CURNUTTE, B., *J. Quant. Spectrosc. Radiat. Transfer* **2** (1962) 41.
[3] FIUTAK, J. and VAN KRANENDONK, J., *Can. J. Phys.* **40** (1962) 1085 ; *Can. J. Phys.* **41** (1963) 21.
[4] BIRNBAUM, G., *Adv. Chem. Phys.* **12** (1967) 487.
[5] GRAY, C. G., *J. Chem. Phys.* **61** (1974) 418.
[6] BOULET, C., ROBERT, D. and GALATRY, L., *J. Chem. Phys.* **65** (1976) 5302.
[7] GIRAUD, M., ROBERT, D. and GALATRY, L., *J. Chem. Phys.* **51** (1969) 2192.
[8] VARANASI, P. and SARANGI, S., *J. Quant. Spectrosc. Radiat. Transfer* **14** (1974) 845.
[9] TIPPING, R. H. and HERMAN, R. M., *J. Quant. Spectrosc. Radiat. Transfer* **10** (1970) 881.
[10] JARECKI, J. and HERMAN, R. M., *J. Quant. Spectrosc. Radiat. Transfer* **15** (1975) 707.
[11] JARECKI, J., *J. Chem. Phys.* **65** (1976) 5318.
[12] MURPHY, J. S. and BOGGS, J. E., *J. Chem. Phys.* **47** (1967) 691.
[13] SMITH, E. W., GIRAUD, M. and COOPER, J., *J. Chem. Phys.* **65** (1976) 1256.
[14] SMITH, E. W., GIRAUD, M., *J. Chem. Phys.* **66** (1977) 1762.
[15] BOULET, C. and ROBERT, D., *Chem. Phys. Lett.* **60** (1978) 162.
[16] MC GUIRE, P. and KOURI, D. J., *J. Chem. Phys.* **60** (1974) 2488 ; MC GUIRE, P., *Chem. Phys. Lett.* **23** (1973) 575. KOURI, D. J. and MC GUIRE, P., *Chem. Phys. Lett.* **29** (1975) 414.
[17] RABITZ, H., *J. Chem. Phys.* **57** (1972) 1718 ; ZARUR, G. and RABITZ, H., *J. Chem. Phys.* **59** (1973) 943.
[18] VARANASI, P., *J. Quant. Spectrosc. Radiat. Transfer* **14** (1974) 995 ; **15** (1975) 255, and other references of the same author cited in these papers.
[19] LAM, K. S., *J. Quant. Spectrosc. Radiat. Transfer* **17** (1977) 351.
[20] TEJWANI, G. D. T. and YEUNG, E. S., *J. Chem. Phys.* **66** (1977) 4915.
[21] SRIVASTAVA, G. P., KUMAR, D. and KUMAR, A., *J. Chem. Phys.* **66** (1977) 20.
[22] BONAMY, J. and ROBERT, D., *J. Quant. Spectrosc. Radiat. Transfer* **15** (1975) 855.
[23] YAMAMOTO, Y., TANAKA, M. and AOKI, T., *J. Quant. Spectrosc. Radiat. Transfer* **9** (1969) 371 ; YAMAMOTO, Y. and CATTANI, M., *J. Quant. Spectrosc. Radiat. Transfer* **20** (1978) 271.
[24] DION, P. and MAY, A. D., *Can. J. Phys.* **51** (1973) 36.
[25] WITKOWICZ, T. and MAY, A. D., *Can. J. Phys.* **54** (1976) 575.
[26] MAY, A. D., VARGHESE, G., STRYLAND, J. C. and WELSH, H. L., *Can. J. Phys.* **42** (1964) 1058.
[27] BURCH, D. E., *J. Opt. Soc. Am.* **58** (1968) 1383.
[28] ROSENKRANZ, P. W., *I.E.E.E. Trans. Antennas Propag.* **23** (1975) 498.
[29] FANO, U., *Phys. Rev.* **141** (1966) 34.
[30] BEN REUVEN, A., *Phys. Rev.* **145** (1966) 7 ; *Phys. Rev.* **141** (1966) 34.
[31] CHERKASOV, M. R., *Opt. Spektrosk.* **40** (1976) 7.
[32] ROSE, M. E., *Elementary theory of Angular Momentum* (John Wiley and Sons), fifth printing, February, 1967.
[33] BARANGER, M., *Phys. Rev.* **111** (1958) 481 ; **111** (1958) 494 ; **112** (1958) 855.
[34] KOLB, A. C. and GRIEM, H., *Phys. Rev.* **111** (1958) 514.
[35] KUBO, R., *Fluctuation, Relaxation and Resonance in Magnetic Systems*, edited by ter Haar (Oliver and Boyd, London) 1962.
[36] BLOCH, C., *Nucl. Phys.* **7** (1958) 451.
[37] HERMAN, R. M., *Phys. Rev.* **132** (1963) 262.
[38] MITHROTRA, S. C. and BOGGS, J. E., *J. Chem. Phys.* **58** (1977) 5306.
[39] BONAMY, J., BONAMY, L. and ROBERT, D., *J. Chem. Phys.* **67** (1977) 4441.
[40] VAN DEN HOUT, K. D., Ph. D. Thesis, Gravenhage, The Netherlands (1978).

[41] GERSTEN, J. I., *Phys. Rev.* A **4** (1971) 98.
[42] BERARD, M. and LALLEMAND, P., *J. Quant. Spectrosc. Radiat. Transfer* **19** (1978) 387.
[43] NEILSEN, W. B. and GORDON, R. G., *J. Chem. Phys.* **58** (1973) 4149.
[44] GIRAUD, M. and ROBERT, D., *Chem. Phys. Lett.* **2** (1968) 551.
[45] TAPIA, O., BESSIS, G. and BRATOZ, S., *Int. J. Quantum Chem.* **4** (1971) 289.
[46] PATCH, R. W., NASA TN D-5486 (1969).
[47] GORDON, R. and KIM, Y., *J. Chem. Phys.* **56** (1972) 3122; **60** (1974) 1842.
[48] PACK, R., *J. Chem. Phys.* **61** (1974) 2091;
PARKER, G. A., SNOW, R. L. and PACK, R. T., *J. Chem. Phys.* **64** (1976) 1668.
[49] RAE, A., *Chem. Phys. Lett.* **18** (1973) 574
[50] GREEN, S., *J. Chem. Phys.* **60** (1974) 2654; **67** (1977) 715 and references cited herein.
[51] SWEET, J. R. and STEELE, W. A., *J. Chem. Phys.* **47** (1967) 3022.
[52] MACRURY, T. B., STEELE, W. A. and BERNE, B. J., *J. Chem. Phys.* **64** (1976) 1288 and references cited herein concerning the *atomic* model.
[53] OOBATAKE, M. and OOI, T., *Prog. Theor. Phys.* **48** (1972) 2132.
[54] KIHARA, T., *Rev. Mod. Phys.* **25** (1953) 831; *Adv. Chem. Phys.* **5** (1963) 147;
KIHARA, T. and KOBA, S., *J. Phys. Soc. Japan* **14** (1959) 247;
KOBA, S., *J. Phys. Soc. Japan* **16** (1961) 627;
KOIDE, A. and KIHARA, T., *Chem. Phys.* **5** (1974) 34.
[55] BERNE, B. J. and PECHUKAS, P., *J. Chem. Phys.* **56** (1972) 4213.
[56] DYMOND, J. H. and SMITH, E. B., *Tables of Virial Coefficients of Gases. A critical compilation* (Clarendon, Oxford) 1969.
[57] KELLEY, K. K., *Bull. U.S. Bur. Mines* **383** (1935).
[58] JORDAN, T. H., SMITH, H. W., STREITS, W. E. and LIPSCOMB, W. N., *J. Chem. Phys.* **41** (1964) 756.
SCHUCH, A. F. and MILLS, R. L., *J. Chem. Phys.* **52** (1970) 6000;
KUAN, T. S., WARSCHEL, A. and SCHNEPP, O., *J. Chem. Phys.* **52** (1970) 3012.
[59] MANNICK, L., STRYLAND, J. C. and WELSH, H. L., *Can. J. Phys.* **49** (1971) 3056.
[60] QUENTREC, B. and BROT, C., *J. Chem. Phys.* **54** (1971) 3655; BAROJAS, J., LEVESQUE, D. and QUENTREC, B., *Phys. Rev.* A **7** (1973) 1092.
[61] HIRSCHFELDER, J. O., CURTISS, C. F. and BIRD, R. B., *Molecular Theory of Gases and Liquids* (Wiley, New York, 1954, fourth printing) 1967.
[62] BILLINGSLEY, F. P. and KRAUSS, M., *J. Chem. Phys.* **60** (1974) 2767.
[63] BONAMY, J. and ROBERT, D., *J. Quant. Spectrosc. Radiat. Transfer* **16** (1976) 185;
BONAMY, J., Thèse, Besançon (1977).
[64] GIRAUD, M., ROBERT, D. and GALATRY, L., *J. Chem. Phys.* **59** (1973) 2204.
[65] BOUANICH, J. P. and HAEUSLER, C., *J. Quant. Spectrosc. Radiat. Transfer* **12** (1972) 695.
[66] DOWLING, J. M., *J. Quant. Spectrosc. Radiat. Transfer* **9** (1969) 1613.
[67] BOUANICH, J. P. and BRODBECK, C., *J. Quant. Spectrosc. Radiat. Transfer* **13** (1973) 1.
[68] JAMMU, K. S., St JOHN, G. E. and WELSH, H. L., *Can. J. Phys.* **44** (1966) 797.
[69] VAN KRANENDONK, J., *Can. J. Phys.* **41** (1963) 433.
[70] GRAY, C. G. and VAN KRANENDONK, J., *Can. J. Phys.* **44** (1966) 2411.
[71] VARANASI, P., *J. Quant. Spectrosc. Radiat. Transfer* **15** (1975) 191.
[72] DRAEGERT, D. A. and WILLIAMS, D., *J. Opt. Soc. Am.* **58** (1968) 1399.
[73] VARANASI, P. and TEJWANI, G. D. T., *J. Quant. Spectrosc. Radiat. Transfer* **11** (1971) 255.